Earth Syst. Dynam. Discuss., https://doi.org/10.5194/esd-2017-85
Manuscript under review for journal Earth Syst. Dynam.
Discussion started: 3 November 2017

Earth System Dynamics
Open Access
Discussions

Global meteorological drought and severe drought affected population in 1.5°C and 2°C warmer worlds

Wenbin Liu[a], Fubao Sun[a,b,c,d*], Wee Ho Lim[a,e], Jie Zhang[a], Hong Wang[a], Hideo Shiogama[f] and Yuqing Zhang[g]

[a] Key Laboratory of Water Cycle and Related Land Surface Processes, Institute of Geographic Sciences and Natural Resources Research, Chinese Academy of Sciences, Beijing, China
[b] Ecology Institute of Qilian Mountain, Hexi University, Zhangye, China
[c] College of Resources and Environment, University of Chinese Academy of Sciences, Beijing, China
[d] Center for Water Resources Research, Chinese Academy of Sciences, Beijing, China
[e] Environmental Change Institute, University of Oxford, Oxford, UK
[f] Center for Global Environmental Research, National Institute for Environmental Studies, Tsukuba, Japan
[g] College of Atmospheric Sciences, Nanjing University of Information Science and Technology, Nanjing, China

Corresponding to: Prof. Fubao Sun (*sunfb@igsnrr.ac.cn*), Institute of Geographic Sciences and Natural Resources Research, Chinese Academy of Sciences

Earth Syst. Dynam. Discuss., https://doi.org/10.5194/esd-2017-85
Manuscript under review for journal Earth Syst. Dynam.
Discussion started: 3 November 2017

Abstract. In Paris Agreement of 2015, a more ambitious climate change mitigation target, on limiting the global warming at 1.5°C instead of 2°C above pre-industrial levels, has been proposed. Scientific investigations are necessary to investigate environmental risks associated with these warming targets. This study is the first risk-based assessment of changes in global meteorological drought and the impact of severe drought on population at 1.5°C and 2°C additional warming conditions using the CMIP5 (the fifth Coupled Model Intercomparison Project) climate models. Our results highlight the risk of meteorological drought at the globe and in several hotspot regions such as Amazon, Northeastern Brazil, South Africa and Central Europe at both 1.5 °C and 2 °C global warming relative to the historical period. Correspondingly, more people would be exposed to severe droughts in many regions (i.e., total and urban population in East Asia, Southeast Asia, Central Europe and rural population in Central Asia, South Africa and South Asia). By keeping the warming at 1.5°C above the pre-industrial levels instead of 2°C, the risks of meteorological drought would decrease (i.e., less drought duration, drought intensity and drought severity but relatively more frequent severe drought) and the affected total and urban population would decrease (the exposed rural population would increase in most regions) at global and sub-continental scales. Whilst challenging for the rural areas, the benefits of limiting warming to below 1.5°C are significant for reducing the risks and societal impacts of global meteorological drought.

1 Introduction

Drought is a major natural hazard which could lead to adverse impacts consequences on water supplies, food productions and the environment (Wang et al., 2011; Sheffield et al., 2012).

Because of these serious consequences, the occurrence of severe droughts has gained wide attentions, these include the Millennium drought in southeast Australia (van Dijk et al., 2013; Kiem et al., 2016), the once-in-a-century droughts in southwest China (Qiu, 2010, Zuo et al., 2015), the Horn of Africa drought (Masih et al., 2014; Lyon, 2014) and the recent California drought (Aghakouchak et al., 2015; Cheng et al., 2016). In the context of climate change, drought risks (i.e., drought duration and intensity) are likely to increase in many historical drought-prone regions with global warming (Dai et al., 2012; Fu and Feng, 2014; Kelley et al., 2015; Ault et al., 2016). A better understanding of changes in global drought characteristics and their socioeconomic impacts in the 21st century should feed into long-term climate adaptation and mitigation plans.

The United Nations Framework Convention on Climate Change (UNFCCC) agreed to establish a long-term temperature goal for climate projection of "*pursue efforts to limit the temperature increase to 1.5°C above pre-industrial levels, recognizing that this would significantly reduce the risks and impacts of climate change*" (UNFCCC Conference of the Parties, 2015) in the 2015 Paris Agreement, and invited the Intergovernmental Panel on Climate Change (IPCC) to announce a special report "*On the impacts of global warming of 1.5°C above pre-industrial levels and related greenhouse gas emission pathways*" in 2018 (Mitchell et al., 2016). Regardless of the socio-economic and political achievability of this goals (Sanderson et al., 2017), there is a paucity of scientific knowledge about the relative risks (i.e., drought risks and their potential impacts) associated with the implications of 1.5°C and/or 2°C warming, this naturally attracted contributions from scientific community (Hulme 2016, Schleussner et al., 2016, Peters 2016, King et al., 2017).

To target on the impact assessments of 1.5°C and/or 2°C warming, there are currently several approaches (James et al., 2017). For example, (1) to enable impact assessments at near-equilibrium climate of 1.5°C and/or 2°C warmer worlds designed specifically using a set of ensemble simulations with a coupled climate model (i.e., Community Earth System Model, CESM) (Sanderson et al., 2017; Wang et al., 2017). Although similar results of drought response to warming were obtained as that conducted by Coupled Model Intercomparison Project-style experiments (i.e., CMIP5, Taylor et al., 2012), the structural uncertainty and robustness of change in droughts among different models cannot be fully evaluated in this kind of single-model study (Lehner et al., 2017). (2) The HAPPI (Half a degree Additional warming, Projections, Prognosis and Impacts) model intercomparison project provided a new assessment framework and a dataset with experiment design target explicitly to 1.5°C and 2°C above the pre-industrial levels (Mitchell et al., 2017). However, the analysis/calculation of meteorological drought characteristics needs data with longer duration (typically >20 consecutive years), the ten-year period HAPPI dataset (i.e., 2005-2016 for the historical period and 2105-2116 for the 1.5°C and 2°C warmer worlds) is relatively short (consecutive samples are too short for calculating a drought index, i.e., Palmer drought severity index, PDSI, Palmer, 1965) for an index-based meteorological drought assessment. (3) Outputs from CMIP5 climate models under the RCP2.6 scenarios were also applied for this kind of "risk assessment-style" studies, but only a handful of General Circulation Models (GCMs) simulations end up showing 1.5°C global warming by end of the 21st century. Alternatively, transient simulations from multiple CMIP5 GCMs at higher greenhouse emissions

Earth Syst. Dynam. Discuss., https://doi.org/10.5194/esd-2017-85
Manuscript under review for journal Earth Syst. Dynam.
Discussion started: 3 November 2017

Earth System Dynamics Discussions Open Access EGU

(i.e., the RCP4.5 and RCP8.5) (Schleussner et al., 2016; King et al., 2017) could be analyzed in order to evaluate the potential risks of meteorological drought under different warming targets, albeit the long-duration drought years might be underestimated due to insufficient sampling of extended drought events (Lehner et al., 2017).

Here, we quantify the changes in global and sub-continental meteorological drought characteristics (i.e., drought duration, intensity and severity) at 1.5°C and 2°C above the pre-industrial levels and whether there are significant differences between them. We perform this analysis using a drought index-PDSI forced by a suite of latest CMIP5 GCMs. To evaluate the societal impacts, we incorporate the Shared Socioeconomic Pathway 1 (SSP1) spatial explicit global population scenario and examine the exposure of population (including rural, urban and total population) to severe drought events. This paper is organized as follows: Section 2 introduces the CMIP5 GCMs output and SSP1 population data applied in this study. The definition of the baseline period, 1.5°C and 2°C warmer worlds, and the calculation of PDSI-based drought characteristics and population exposed to severe drought are also described in this section. Section 3 shows the results (i.e., hotspots and risks) of changes in drought characteristics and the impacts of severe drought on people under these warming targets. Detailed discussions are performed in Section 4, followed by the conclusions in Section 5.

2 Material and Methods

2.1 Data

Earth Syst. Dynam. Discuss., https://doi.org/10.5194/esd-2017-85
Manuscript under review for journal Earth Syst. Dynam.
Discussion started: 3 November 2017

Earth System Dynamics
Discussions
Open Access

In this study, we use the CMIP5 GCMs output (including the monthly outputs of surface mean air temperature, surface minimum air temperature, surface maximum air temperature, air pressure, precipitation, relatively humidity, surface downwelling longwave flux, surface downwelling shortwave flux, surface upwelling longwave flux and surface upwelling shortwave flux as well as the daily outputs of surface zonal velocity component ($uwnd$) and meridional velocity component ($vwnd$)) under two Representative Concentration Pathways (RCP4.5 and RCP8.5) archived at the Earth System Grid Federation (ESGF) Node at the German Climate Computing Center-DKRZ (https://esgf-data.dkrz.de/projects/esgf-dkrz/) over the period 1850-2100. Based on data availability, we select 11 GCMs to perform the analysis (see details of these GCMs in Table 1). In the CMIP5 archive, the monthly $uwnd$ and $vwnd$ were computed as the means of their daily values with the plus-minus sign, the calculated wind speed from the monthly $uwnd$ and $vwnd$ would be equal to or, in most cases, less than that computed from the daily values (Liu and Sun, 2016). To get the monthly wind speed, we average the daily values ($\sqrt{uwnd^2 + vwnd^2}$) over a month. We rescale all data to a common spatial resolution of $0.5^{\circ} \times 0.5^{\circ}$ using the bilinear interpolation.

<Table 1, here, thanks>

To consider the people affected by severe drought events, we use the spatial explicit global population scenarios developed by researchers from the Integrated Assessment Modeling (IAM) group of National Center for Atmospheric Research (NCAR) and the City University of New York Institute for Demographic Research (Jones and O'Neil, 2016). They included the gridded population data for the baseline year (2000) and for the period of 2010-2100 in ten-year steps at a spatial resolution of 0.125 degree, which are consistent with the new Shared Socioeconomic

Earth Syst. Dynam. Discuss., https://doi.org/10.5194/esd-2017-85
Manuscript under review for journal Earth Syst. Dynam.
Discussion started: 3 November 2017

Earth System Dynamics
Open Access
Discussions

Pathways (SSPs). We apply the population data of the SSP1 scenario, which describes a future pathway with sustainable development and low challenges for adaptation and mitigation. We upscale this product to a spatial resolution of 0.5° ×0.5°. For the global and sub-continental scales analysis, we use the global land mass between 66°N and 66°S (Fischer et al., 2013; Schleussner et al., 2016) and 26 sub-continental regions (as used in IPCC, 2012, see Table 2 for details).

<Table 2, here, thanks>

2.2 Definition of a baseline, 1.5°C and 2°C worlds

To define a baseline, 1.5°C and 2°C worlds, we first calculate the global mean surface air temperature (GMT) for each climate model and emission scenario over the period 1850-2100. We note that the surface air temperature field need be weighted by the square root of cosine (latitude) to consider the dependence of grid density on latitude (Liu et al., 2016). The Multi-model Ensemble Mean (MEM) GMT were computed and smoothed using a 20-year moving average filter for the RCP4.5 and RCP8.5 scenarios, respectively. Following the method in Wang et al. (2017), we select a baseline period of 1986-2005 when the observed GMT was 0.6°C warmer (the MEM GMT was 0.4~0.8 $^{\circ}$C warmer during this period in 11 climate models used) than the pre-industrial levels (1850-1900, IPCC, 2013). This is also a common reference period for climate impact assessment (e.g., Schleussner et al., 2016). Next, for each emission scenario (RCP4.5 or RCP8.5), we define the periods (Figure 1) during which the 20-year smoothed GMT increase by 1.3~1.7 $^{\circ}$C (2027-2038 under the RCP4.5 and 2029-2047 under the RCP 8.5) and by 1.8~2.2 $^{\circ}$C (2053-2081 under the RCP4.5 and 2042-2053 under the RCP 8.5) above the pre-industrial period as the 1.5°C and 2°C warming worlds, respectively (as in King et al., 2017). To reduce the projection uncertainty inherited from different emission scenarios, we combine (average) the

Earth Syst. Dynam. Discuss., https://doi.org/10.5194/esd-2017-85
Manuscript under review for journal Earth Syst. Dynam.
Discussion started: 3 November 2017

results of drought characteristics and population exposures calculated during different selected periods under the RCP4.5 and RCP8.5, to represent the ensemble means meteorological drought risk at 1.5°C or 2°C warmer worlds.

<Figure 1, here, thanks>

2.3 Characterize meteorological drought using PDSI

To quantify the changes in drought characteristics, we adopt the most widely used PDSI index, which describes the balance between water supply (precipitation) and atmospheric evaporative demand (required “precipitation” estimated under climatically appropriate for existing conditions, CAFEC) at the monthly scale (Zhang et al., 2016). Briefly, it incorporates antecedent precipitation, potential evaporation and the local Available Water Content (AWC, links: https://daac.ornl.gov/cgi-bin/dsviewer.pl?ds_id=548) of the soil in the hydrological accounting system. It measures the cumulative departure relative to the local mean conditions in atmospheric moisture supply and demand on land surface. In the PDSI model, five surface water fluxes, namely, precipitation (*P*), recharge to soil (*R*), actual evapotranspiration (*E*), runoff (*RO*) and water loss to the soil layers (*L*); and their potential values $\hat{P}$, *PR*, *PE*, *PRO* and *PL* are considered. All values in the model can be computed under CAFEC values using the precipitation, potential evaporation and AWC inputs. For example, the CAFEC precipitation ($\hat{P}$) is defined as (Dai et al., 2011),

$$\hat{P}=\frac{\overline{E_i}}{\overline{PE_i}}PE+\frac{\overline{R_i}}{\overline{PR_i}}PR+\frac{\overline{RO_i}}{\overline{PRO_i}}PRO-\frac{\overline{L_i}}{\overline{PL_i}}PL, \qquad (1)$$

Here the over bar indicates averaging of a parameter over the calibration period. The moisture anomaly index (*Z* index) is derived as the product of the monthly moisture departure ($P-\hat{P}$) and a climate characteristics coefficient *K*. The *Z* index is then applied to calculate the PDSI value for time $t(X_t)$:

$$X_t = pX_{t-1} + qZ_t = 0.897X_{t-1} + Z_t/3 \tag{2}$$

Where X_{t-1} is the PDSI of the previous month, and p and q are duration factors. The calculated PDSI ranges -10 (dry) to 10 (wet). Details of PDSI are available in Palmer (1965) and Wells et al. (2004).

As part of the PDSI calculation, we calculate the potential evaporation (PET) using the Food and Agricultural Organization (FAO) Penman-Monteith equation (Allen et al., 1998),

$$PET = \frac{0.408\Delta(R_n - G) + \gamma\frac{900}{T+273}U_2 e_s(1 - \frac{Rh}{100})}{\Delta + \gamma(1 + 0.34U_2)} \tag{3}$$

where Δ is the slope of the vapor pressure curve, U_2 is the wind speed at 2 m height, G is the soil heat flux, Rh is the relative humidity, γ is the psychometric constant, e_s is the saturation vapor pressure at a given air temperature (T). R_n is the net radiation which can be calculated using the surface downwelling/upwelling shortwave and longwave radiations. We estimate all other parameters in the FAO Penman-Monteith equation using the GCM outputs through the standard algorithm as per recommended by the FAO (Allen et al., 1998). In this study, we perform this calculation for each GCM over the period 1850-2100 using the tool for calculating the Palmer drought indices (the original MATLAB codes were modified for this case) developed by Jacobi et al. (2013).

Based on the calculated global PDSI, we derive the drought characteristics (i.e., drought duration, drought intensity and drought severity) using the run theory for the baseline, 1.5°C and 2°C warming worlds, respectively. Briefly, the concept of "run theory" is proposed by Yevjevich and Ingenieur (1967). The run characterizes the statistical properties of sequences in both time and space. It is useful for defining drought in an objective manner. In the run theory, a "run" represents a portion of time series X_i, where all values are either below or above a specified threshold (we set the threshold PDSI < -1 in this study) (Ayantobo et al., 2017). We define a "run" with values continuously stay below that threshold (i.e., negative run) as a drought event, which generally includes these characteristics: drought duration, drought intensity and drought severity (see Figure 2 for better illustration). We define the drought duration as a period (years/months/weeks) which PDSI stays below a specific threshold. Drought severity indicates a cumulative deficiency of a drought event below the threshold, while drought intensity is the average value of a drought event below the threshold (Mishra and Singh, 2010). For each GCM, we calculate the medians of drought duration, drought intensity and drought severity at each grid-cell across all drought events for each selected period (i.e., the baseline, 1.5°C and 2°C warming worlds). We generalize the results by evaluating the ensemble mean and model consistency/inter-model variance across all climate models.

<Figure 2, here, thanks>

2.4 Calculation of population exposure to severe droughts

Following Wells et al. (2014), we assume that a severe drought event occurs when monthly PDSI < -3. If a severe drought occurs for at least a month in a year, we would take that year as a severe drought year. For each GCM per period (i.e., the baseline, 1.5°C and 2°C warming worlds), we quantify the population (including urban, rural and all population) affected by severe drought per grid-cell as (population × annual frequency of severe drought). We first compute the affected population using the SSP1 data (see Section 2.1). For example, we used the SSP1 base year (2000), 2030 (centered year in the 1.5°C warming period: 2027-2047 for both RCP scenarios) and 2060 (centered year in the 2°C warming period: 2042-2081 for both RCP scenarios) population data for the baseline period (1985-2005), 1.5°C and 2°C warming worlds, respectively. To evaluate the climate impact on society without population growth, we estimate the population exposure using the SSP1 data of the base year (2000). We repeat this estimation using the constant SSP1 population data in 2100, which is consistent with the original proposal of Paris Agreement on stabilizing global warming for the specified targets by end of the 21st century.

3 Results

3.1 Changes in PDSI and drought characteristics

We present the changes in multi-model ensemble mean PDSI from the baseline period (1986-2005) to each of the 1.5°C and 2°C scenarios and model consistency in Figure 3. For the 1.5°C warmer world, the PDSI would decrease (drought-prone) with relatively higher model consistency (6~11 models in totally 11 climate models) in some regions, for example, Amazon (0.7±0.8 -> -0.1±0.2), Northeastern Brazil (0.5±0.6 -> -0.1±0.3), Southern Europe and Mediterranean (0.4±0.6 -> -0.3±0.2), Central America and Mexico (0.2±0.4 -> -0.2±0.1), Central Europe (0.3±1.0 -> -0.1±0.4) as well as Southern Africa (0.5±0.5 -> -0.3±0.2); slightly increase (less drought-prone) in Alaska/Northwest Canada (-0.01±0.5 -> -0.3±0.2) and North Asia (-0.1±1.0 -> -0.2±0.2) but with relatively low model consistency. The geographic pattern of changes in PDSI for the 2°C scenario is quite similar to that of 1.5°C warmer world, but the magnitude of change

Earth Syst. Dynam. Discuss., https://doi.org/10.5194/esd-2017-85
Manuscript under review for journal Earth Syst. Dynam.
Discussion started: 3 November 2017

would intensify (in both direction) East Canada, Greenland, Iceland (-0.3±0.2-> -0.4±0.2), East Africa (-0.5±0.2-> -0.3±0.2), Northern Europe (-0.3±0.3-> -0.2±0.3), East Asia (-0.3±0.1-> -0.2±0.4), South Asia (-1.0±1.2-> -0.8±0.3) and West Africa (-0.3±0.2-> -0.3±0.3). When global warming is kept at 1.5°C instead of 2°C above the pre-industrial levels, the PDSI value would be larger at the globe (66°S-66°S, -0.4±0.2-> -0.3±0.2) and most regions (Alaska/Northwest Canada, East Africa, West Africa, Tibetan Plateau, North Asia, East Asia, South Asia and Southeast Asia) (Figure 4).

<Figure 3, here, thanks>

<Figure 4, here, thanks>

We analyze the changes in meteorological drought characteristics such as it duration, severity and intensity under the 1.5°C and 2°C warming conditions. In terms of the drought duration (Figure 5 and Figure 6), we find robust large-scale features. For example, the drought duration would generally increase at the globe (2.9±0.5 -> 3.1±0.4 months and 2.9±0.5 -> 3.2±0.5 months from the baseline period to the 1.5°C and 2°C scenarios) and most regions (especially for Amazon, Sahara, Northeastern Brazil and North Australia) except for North Asia (2.7±0.6 -> 2.6±0.5 months and 2.7±0.6 -> 2.5±0.4 months) under both the 1.5°C and 2°C warmer worlds. The high model consistency in most regions (i.e., Amazon, Sahara and Northeastern Brazil) for both warming scenarios gives us more confidence on these projections. Relative to the 2°C warmer target, a 1.5°C warming target is more likely to reduce drought duration at both global and regional scales (except for Alaska/Northwest Canada, East Africa, Sahara, North Europe, North Asia, South Asia, Southeast Asia, Tibetan Plateau and West Africa).

<Figure 5, here, thanks>

<Figure 6, here, thanks>

Earth Syst. Dynam. Discuss., https://doi.org/10.5194/esd-2017-85
Manuscript under review for journal Earth Syst. Dynam.
Discussion started: 3 November 2017

Drought intensity and drought severity are commonly used for quantifying, to what extent, the water availability significantly below normal conditions for a region. In this study, the drought intensity is projected to increase at the globe (0.9±0.3 -> 1.1±0.3 and 0.9±0.3 -> 1.0±0.2 from the baseline period to the 1.5^{o}C and 2^{o}C scenarios) and in most of the regions except for North Asia, Southeast Asia and West Africa under the 1.5^{o}C and 2^{o}C warming scenarios (Figures 7-8). Compare to the 2^{o}C scenario, the drought intensity would obviously be relieved at the global and sub- continental scales except for East Canada, Greenland, Iceland (1.0±0.6 -> 0.8±0.5) and West North America (0.9±0.3 -> 0.8±0.2) in the 1.5^{o}C warmer world. In addition, the projected drought severity would also increase in both 1.5^{o}C and 2^{o}C warmer worlds at the globe (3.0±1.9 -> 4.5±3.0 and 3.0±1.9 -> 3.8±2.0 from the baseline period to the 1.5^{o}C and 2^{o}C scenarios) and in most regions except for North Asia (1.8±0.6 -> 1.8±0.7 and 1.8±0.6 -> 1.5±0.3) (Figures 9-10). When global warming is maintained at 1.5^{o}C instead of 2^{o}C above the pre-industrial levels, the drought severity would weaken in most regions except for Sahara (3.1±0.9-> 3.5±1.3), North Asia (1.5±0.3 -> 1.8±0.8), Southeast Asia (17.2±20.1 -> 35.8±57.2), and West North America (2.4±1.7 -> 2.5±1.4).. The projected uncertainties are relatively low (6~11 models in totally 11 models) for the changes of each drought character under different warming scenarios all over the world except for some parts of Alaska/Northwest Canada, East Canada, Greenland, Iceland, West North America, Central North America, East North America, Sahara, West Africa, East Africa and North Asia.

<Figure 7, here, thanks>

<Figure 8, here, thanks>

3.2 Impact of severe drought on population

Earth Syst. Dynam. Discuss., https://doi.org/10.5194/esd-2017-85
Manuscript under review for journal Earth Syst. Dynam.
Discussion started: 3 November 2017

Earth System Dynamics Discussions Open Access

To understand the societal influences of severe drought, we combine the drought projection with SSP1 population information and estimate the total, urban and rural population affected by severe drought in the baseline period, 1.5°C and 2°C warmer worlds (Figures 11-13). Compare to the baseline period, the frequency of severe drought (PDSI < -3), drought-affected total and urban population would increase in most of the regions under the 1.5°C and 2°C warming scenarios.

<Figure 9, here, thanks>

<Figure 10, here, thanks>

The projections suggest that more urban population would expose to severe drought in Central Europe (16.4±8.5 million), Southern Europe and Mediterranean (13.3±4.7 million), West Africa (26.7±15.7 million), East Asia (44.3±20.6 million), South Asia (17.7±37.6 million), West Asia (14.9±7.8 million) and Southeast Asia (19.9±17.0 million) in the 1.5°C warmer world relative to the baseline period. We also find that the number of affected people would escalate further in these regions under the 2°C warming scenario (Table 3). In terms of the rural population, more people in Central Asia (2.2±6.4 million and 1.2±3.5 million for the 1.5°C and 2°C warmer worlds), Central North America (0.8±1.7 million and 0.4±1.0 million), Southern Europe and Mediterranean (0.9±3.4 million and 0.3±4.9 million), South Africa (1.9±1.9 million and 0.9±2.6 million), Sahara (0.1±2.5 million and 0.3±3.2 million), South Asia (45.9±52.4 million and -23.1±26.9 million), Tibetan Plateau (0.3±2.7 million and -1.03±2.1 million) and West North America (-1.2±0.9 million and 0.1±0.1 million) would expose to the severe drought in the 1.5°C and 2°C warmer worlds relative to the baseline period (except for the globe, South Asia and Tibetan Plateau under the 2°C warming scenario and West North America under the 1.5°C warming scenario). Overall, the

Earth Syst. Dynam. Discuss., https://doi.org/10.5194/esd-2017-85
Manuscript under review for journal Earth Syst. Dynam.
Discussion started: 3 November 2017

multi-model projected uncertainty of affected population (including total, urban and rural population) is quite small in most regions except for East Asia, South Asia and West Africa.

<Figure 11, here, thanks>

<Figure 12, here, thanks>

When global warming approaches 1.5^{o}C (instead of 2^{o}C) above the pre-industrial levels, relatively less total (except for total population affected in North Asia, East Asia, Southeast Asia and South Asia) and urban population would be affected despite more frequent severe drought. By contrast, the affected rural population would increase in most regions (except for Amazon, East Canada, Greenland, Iceland, North Australia, Northeastern Brazil, Sahara and South Australia/New Zealand). This implies that the benefit of holding global warming at 1.5^{o}C instead of 2^{o}C is apparent to the severe-drought affected total and urban population, but challenges remain in the rural areas (especially in South Asia, Southeast Asia, East Africa and West Africa).

<Figure 13, here, thanks>

<Table 3, here, thanks>

We repeat similar analysis using the constant SSP1 population in 2100 (Figure 4). Relative to the baseline period, we find that 38.6±272.7million (38.7±247.1 million urban population and 0.0±26.1million rural population) and 100.3±323.9 million (99.1±295.9 million urban population and 1.5±28.5 million rural population) additional population would expose to severe droughts in the 1.5^{o}C and 2^{o}C warmer worlds on a global scale. The severe drought affected total, urban and rural population would increase under these warming targets in most regions except for Sahara (total and rural population under 1.5^{o}C warming scenario and rural population under 2^{o}C warming scenario), East Africa, South Asia and West Africa (rural population under 1.5^{o}C warming scenario). Moreover, compare to the 2°C warming target, the severe drought affected total, urban and rural population would decrease in the 1.5°C warmer world in most regions such as East Asia, Southern Europe and Mediterranean, Central Europe and Amazon.

To exclude the role of population growth in the former analysis, we also repeat the analysis but this time we keep the population constant in 2000 (Table 4). Globally, we estimate that 63.8±195.9 million (33.3±86.6 million urban population and 30.5±113.6 million rural population) and 122.4±249.9 million (55.4±101.8 million urban population and 67.0±150.7 million rural population) additional people would be exposed solely to severe droughts in the 1.5°C and 2°C warmer worlds, respectively. In terms of percentage, about 75% and 50% of total affected population (considers both severe droughts and population growth, including 86% and 88% of the affected urban population as well as 114% and -67% of the affected rural population) are attributable to population growth while others are solely due to climate change impact under the 1.5°C and 2°C warming scenarios, respectively. The climate change driven severe drought affected total, urban and rural population would decrease in East Africa and South Asia but increase (the climate change driven severe drought affected population constitutes >50% of that considering both climate change and population growth) in most regions (for example, North Australia, Southern Europe and Mediterranean, Central Europe, North Europe, West Coast South America, Northeastern Brazil, Central North America and East Asia for total population as well as West North America, Central North America, East North America, Central America and Mexico, Amazon, Northeastern Brazil, West Coast South America, Southeastern South America, Northern Europe, Central Europe, Southern Europe and Mediterranean, West Africa, South Africa, North

Earth Syst. Dynam. Discuss., https://doi.org/10.5194/esd-2017-85
Manuscript under review for journal Earth Syst. Dynam.
Discussion started: 3 November 2017

Asia, Central Asia, Tibetan Plateau, East Asia and Southeast Asia for rural population) under these warming targets.

<Table 4, here, thanks>

4 Discussions

The changes in PDSI, drought duration, intensity and severity with climate warming (i.e., +1.5°C and +2°C warmer worlds) projected in this study is in general agreement with that concluded by IPCC (2013), although they vary among regions. For example, as revealed in this study, the gradual decline of PDSI (drought-prone) in American Southwest and Central Plains was also projected using an empirical drought reconstruction and soil moisture metrics from 17 state–of-the-art GCMs in the 21st century (Cook et al., 2015). The ascending risk of drought in Sahara, North Australia and South Africa coincided with Huang et al. (2017), which projected that global drylands would degrade under the 2°C global warming target. Moreover, the increases in drought duration, intensity and severity in Central America, Amazon, South Africa and Mediterranean are in agreement with the extension of dry spell length and less water availability in these regions under the 1.5°C and/or 2°C warming scenarios (Schleussner et al., 2016; Lehner et al., 2017). In addition, we find that the affected population attributes more (50%~75%) to the population growth rather than the climate change driven severe drought in the 1.5°C and 2°C warmer worlds. This figure is higher than that concluded by Smirnov et al. (2016), maybe due to different study periods, population data, drought index and warming scenarios used.

This study illustrates some of the differences in drought characteristics at both global and sub-continental scales that could be expected in a 1.5°C and 2°C warmer worlds. These projections inherited several sources of uncertainty. Firstly, there are considerable uncertainties in the numerical projections from different climate models under varied greenhouse gas emission scenarios, especially on a regional scale (i.e., Sahara, Alaska/Northwest Canada and North Asia). However, the utility of multiple GCMs and emission scenarios should allow us to generalize future projections than that using single model/scenario (Schleussner et al., 2016; Wang et al., 2017; Lehner et al., 2017). On top of that, we performed uncertainty analysis such as understanding the model consistency (e.g., increase/decrease) and inter-model variance (for magnitude changes). These enable us to characterize regional and global projections which could vary due to different model structure of GCMs and how they behave under different RCP scenarios. Secondly, there are various ways of picking the 1.5°C or 2°C warming signals (King et al., 2017). In this study, we consider both the influences of multi-model and multi-scenario for each warming scenario using the 20-year smoothed multi-model ensemble mean GMT. The selected period of 1.5°C and/or 2.0°C world is close to that of King et al.(2017). Finally, the SSP1 population data and the single drought index used might introduce uncertainties. Despite these sources of uncertainty, these projections are quite robust with high model consistency across most regions.

5 Conclusions

Based on the CMIP5 GCMs output, we presented the first comprehensive assessment of changes in meteorological drought characteristics and the potential impacts of severe drought on population (total, urban and rural) under the 1.5°C and 2°C warmer worlds. We found that the risk of meteorological drought would increase (i.e., decrease in PDSI, increase in drought duration, drought intensity and drought severity) globally and most regions (i.e., Amazon, Northeastern

Earth Syst. Dynam. Discuss., https://doi.org/10.5194/esd-2017-85
Manuscript under review for journal Earth Syst. Dynam.
Discussion started: 3 November 2017

Brazil, Central Europe) for both 1.5°C and 2°C warming scenarios relative to the baseline period (1986-2005). However, the amplitudes of change in drought characteristics vary among the regions. Relative to the 2°C warming target, a 1.5°C warming target is more likely to reduce drought risk (less drought duration, drought intensity and drought severity but relatively more frequent severe drought) significantly on both global and regional scales. The high model consistency (6~11 out of 11 GCMs) across most regions (especially Amazon, Sahara and Northeastern Brazil) gives us more confidence on these projections.

Despite the uncertainties inherited from the GCMs and population data used, as well as the definition of the 1.5°C and 2°C periods, we found significant changes of drought characteristics under both warming scenarios and societal impacts of severe drought by limiting temperature target at 1.5 °C instead of 2 °C in several hotspot regions. More total (+259.3±238.1 million and +245.8±331.1 million globally) and urban population (+232.6±124.8 million and +468.3±228.0 million globally) would exposed to severe drought in most regions (especially East Asia, Southeast Asia and Central Europe) for both 1.5 °C and 2 °C warming scenarios, particularly for the latter case. Meanwhile, more rural population (+26.7±119.0 million and -99.3±100.2million globally) in Central Asia, East Canada, Greenland, Iceland, Central North America, Southern Europe and Mediterranean, North Australia, South Africa, Sahara, South Asia, Tibetan Plateau and West North America would be affected. When global mean temperature increased by 1.5 °C instead of 2 °C above the pre-industrial level, the total (except for the global scale which would increase by ~5.5%) and urban population (would decrease by ~50.3% globally) affected by severe drought would decline but the affected rural population (would increase by ~73.1% globally) would increase in most regions. This means that local governments should be prepared to deal with meteorological drought-driven challenges in the rural areas (especially in South Asia, Southeast Asia, East Africa and West Africa) relative to the urban areas.

Data availability. The datasets applied in this study are available at the following locations:

- CMIP5 model experiments (Taylor et al., 2012), https://esgf-data.dkrz.de/projects/esgf-dkrz/
- Spatial population scenarios (Shared Socioeconomic Pathway 1, SSP1, Jones and O'Niell, 2016), https://www2.cgd.ucar.edu/sections/tss/iam/spatial-population-scenarios

Competing interests. The authors declare that they have no conflict of interest.

Acknowledgements. This study was financially supported by the National Research and Development Program of China (2016YFA0602402 and 2016YFC0401401), the National Natural Sciences Foundation of China (41401037), the Key Research Program of the Chinese Academy of Sciences (ZDRW-ZS-2017-3-1), the CAS Pioneer Hundred Talents Program (Fubao Sun) and the CAS President's International Fellowship Initiative (Wee Ho Lim, 2017PC0068).

References

Aghakouchat, A., Cheng L., Mazdiyasni, O., and Farahmand, A.: Global warming and changes in risk of concurrent climate extremes: insights from the 2014 California drought, Geophys. Res. Lett., 41, 8847-8852, doi:10.1002/2014GL062308, 2015.

Allen, R., Pereira, L.S., Raes, D., and Smith, M.: Crop evapotranspiration guidelines for computing crop water requirements-FAO Irrigation and drainage paper 56, FAO-Food and Agriculture Organization of the United Nations, Rome, 1998.

Ault, T.R., Mankin, J.S., Cook, B.I., and Smerdon, J.E.: Relative impacts of mitigation, temperature, and precipitation on 21st-century megadrought risk in the American Southwest, Sci. Adv., 2, 1-9, doi:10.1126/sciadv.1600873, 2016.

Ayantobo, O.O., Li, Y., Song, S.B., and Yao, N.: Spatial comparability of drought characteristics and related return periods in mainland China over 1961-2013, J. Hydrol., 550, 549-567, doi:10.1016/j.jhydrol.2017.05.019, 2017.

Cheng, L., Hoerling, M., Aghakouchak, A., Livneh, B., Quan, X.W., and Eischeid, J.: How has human-induced climate change affected California drought risk? J. Clim., 29, 111-120, doi:10.1175/JCLI-D-15-0260.1, 2016.

Cook, B,I., Ault, T.R., Smerdon, J.E.: Unprecedented 21st century drought risk in the American Southwest and Central Plains, Sci. Adv., 1, e1400082, 2015.

Dai, A.G.: Characteristics and trends in various forms of the Palmer drought severity index during 1900-2008, J.Geophys.Res., 116, D12115, doi: 10.1029/2010JD015541, 2011.

Dai, A.G.: Increasing drought under global warming in observations and models, Nat. Clim. Change,3, 52-58, doi: 10.1038/NCLIMATE1633, 2012.

Fischer, E.M., Beyerle, U., and Knutti, R.: Robust spatially aggregated projections of climate extremes, Nat. Clim. Change, 2, 1033-1038, doi:10.1038/nclimate2051, 2013.

Fu, Q., and Feng, S.: Responses of terrestrial aridity to global warming, J. Geophys. Res., 119, 7863-7875, doi: 10.1002/2014JD021608, 2014.

Earth Syst. Dynam. Discuss., https://doi.org/10.5194/esd-2017-85
Manuscript under review for journal Earth Syst. Dynam.
Discussion started: 3 November 2017

Hulme, M.: 1.5°C and climate research after the Paris Agreement, Nat. Clim. Change, 6, 222-224, doi:10.1038/nclimate2939, 2016.

IPCC: Managing the Risks of Extreme Events and Disasters to Advance Climate Change Adaptation, in: A Special Report of Working Group I and II of the Intergovernmental Panel on Climate Change, edited by: Field, C.B., Barros, V., Stocker, T.F., Qin, D., Dokken, D.J., Ebi, K.L., Mastrandrea, M.D., Mach, K.J., Plattner, G.-K., Allen, S.K., Tignor, M., and Midgley, P.M., Cambridge University Press, Cambridge, UK and New York, NY, USA, 582 pp, 2012.

IPCC: Summary for Policymakers, in: Climate Change 2013: The Physical Science Basis, Contribution of Working Group I to the Fifth Assessment Report of the Intergovernmental Panel on Climate Change, edited by: Stocker, T., Qin, D., Plattner, G.-K., Tignor, M., Allen, S., Boschung, J., Nauels, A., Xia, Y., Bex, V., and Midgley, P., IPCC AR WGI, Cambridge University Press, Cambridge, UK and New York, NY, USA, 1-100, 2013.

Jacobi, J., Perrone, D., Duncan, L.L., and Hornberger, G.: A tool for calculating the Palmer drought indices, Water Resour. Res., 49, 6086-6089, doi: 10.1002/wrcr.20342, 2013.

James, R., Washington, R., Schleussner, C.-F., Rogelj, J., and Conway, D.: Characterizing half-a-degree difference: a review of methods for identifying regional climate responses to global warming target, WIREs Clim. Change, 8, e457, doi: 10.1002/wcc.457, 2017.

Jones, B. and O'Neill, B.C.: Spatially explicit global population scenarios consistent with the Shared Socioeconomic Pathways, Environ. Res. Lett., 11, 084003, http://iopscience.iop.org/1748-9326/11/8/084003, 2016.

Earth Syst. Dynam. Discuss., https://doi.org/10.5194/esd-2017-85
Manuscript under review for journal Earth Syst. Dynam.
Discussion started: 3 November 2017

Kelley, C.P., Mohtadi, S., Cane, M.A., Seager, R., and Kushnir, Y.: Climate change in the Fertile Crescent and implications of the recent Syrian drought, Proc. Natl. Acad. Sci., 112, 3241-3246, doi: 10.1073/pnas.1421533112, 2015.

Kiem, A.S., Johnson, F., Westra, S., van Dijk, A., Evans, J.P., O'Donnell, A., Rouillard, A., Barr, C., Tyler, J., Thyer, M., Jakob, D., Woldemeskel, F., Sivakumar, B., Mehrotra, R.: Nature harzards in Australia: drought, Clim. Change, 139, 37-54, doi:10.1007/s10584-016-1798-7, 2016.

King, A.D., Karoly, D.J., and Henley, B.J.: Australian climate extremes at 1.5^{o}C and 2^{o}C of global warming, Nat. Clim. Change, 7, 412-416, doi:10.1038/nclimate3296, 2017.

Lehner, F., Coats, S., Stocker, T.F., Pendergrass, A.G., Sanderson, B.M., Paible, C.C., and Smerdon, J.E.: Projected drought risk in 1.5^{o}C and 2^{o}C warmer climates, Geophys. Res. Lett., 44, 7419-7428, doi:10.1002/2017GL074117, 2017.

Liu, W.B., Lim, W. H., Sun, F.B., Mitchell, D., Wang, H., Chen, D.L., Bethke, I., Shiogama, H., and Fischer, E.: Global freshwater shortage at low runoff conditions based on HAPPI experiments, Envion. Res. Lett., in review, 2017.

Liu, W.B. and Sun, F.B.: Assessing estimates of evaporative demand in climate models using observed pan evaporation over China, J. Geophys. Res. Atmos., 121, 8329-8349, doi: 10.1002/2016JD025166, 2016.

Liu, W.B. and Sun, F.B.: Projecting and attributing future changes of evaporative demand over China in CMIP5 climate models, J. Hydrometeor., 18, 977-991, doi: 10.1175/JHM-D-16-0204.1, 2017.

Earth Syst. Dynam. Discuss., https://doi.org/10.5194/esd-2017-85
Manuscript under review for journal Earth Syst. Dynam.
Discussion started: 3 November 2017

Liu, W.B., Wang, L., Chen, D.L., Tu, K., Ruan, C.Q., and Hu, Z.Y.: Large-scale circulation classification and its links to observed precipitation in the eastern and central Tibetan Plateau, Clim. Dyn., 46(11-12), 3481-3497, doi: 10.1007/s00382-015-2782-z, 2016.

Lyon, B.: Seasonal drought in the Greater Horn of Africa and its recent increase during the march-may long rains, J. Clim., 27, 7953-7975, doi:10.1175/JCLI-D-13-00459.1, 2014.

Masih, I., Maskey, S., Mussá, F.E.F., and Trambauer, P.: A review of droughts on the African continent: a geospatial and long-term perspective, Hydrol. Earth Syst. Sci., 18, 3635-3649, doi:10.5149/hess-18-3635-2014, 2014.

Mishra, A.K. and Singh, V.P.: A review of drought concepts, J. Hydrol., 291, 201-216, doi:10.1016/j.jhydrol.2010.07.012, 2010.

Mitchell, D., James, R., Forster, P.M., Betts, R.A., Shiogama, H., and Allen, M.: Realizing the impacts of a 1.5°C warmer world, Nat. Clim. Change, 6, 735-737, doi:10.10038/nclimate3055, 2016.

Mitchell, D., AchutaRao, K., Allen, M., Bethke, I., Beyerle, U., Ciavarella, A., Forster, P.M., Fuglestvedt, J., Gillett, N., Haustein, K., Ingram, W., Iversen, T., Kharin, V., Klingaman, N., Massey, N., Fischer, E., Schleussner, C.-F., Scinocca, J., Seland, Ø., Shiogama, H., Shuckburgh, E., Sparrow, S., Stone, D., Uhe, P., Wallom, D., Wehner, M., and Zaaboul, R.: Half a degree additional warming, prognosis and projected impacts (HAPPI): background and experimental design, Geosci. Model Dev., 10, 571-583, doi:10.5194/gmd-10-571-2017,2017.

Palmer, W.C.: Meteorological drought, U.S. Department of Commerce Weather Bureau Research, Paper 45, 58 pp., 1965.

Earth Syst. Dynam. Discuss., https://doi.org/10.5194/esd-2017-85
Manuscript under review for journal Earth Syst. Dynam.
Discussion started: 3 November 2017

Peters, G.P.: The "best available science" to inform 1.5°C policy choice, Nat. Clim. Change, 6, 646-649, doi: 10.1038/nclimate3000, 2016.

Qiu, J.: China drought highlights future climate threats, Nature, 465, 142-143, doi:10.1038/465142a, 2010.

Sanderson, B.M., Xu, Y.Y., Tebaldi, C., Wehner, M., O'Neill, B., Jahn, A., Pendergrass, A.G., Lehner, F., Strand, W.G., Lin, L., Knutti, R. and Lamarque, J.F.: Community climate simulations to asses avoided impact in 1.5°C and 2°C futures, Earth Syst. Dyn. Discuss., doi:10.5194/esd-2017-42, 2017.

Schleussner, C., Lissner, T.K., Fischer, E.M., Wohland, J., Perrette, M., Golly, A., Rogelj, J., Childers, K., Schewe, J., Frieler, K., Mengel, M., Hare, W., and Schaeffer, M.: Differential climate impacts for policy-relevant limits to global warming: the case of 1.5°C and 2°C, Earth Syst. Dynam., 7, 327-351, doi: 10.5194/esd-7-327-2016, 2016.

Sheffield, J., Wood, E.F., and Roderick,M.L.: Little change in global drought over the past 60 years, Nature, 491, 435-439, doi:10.1038/nature11575, 2012.

Smirnov, O., Zhang, M.H., Xiao, T.Y., Orbell, J., Lobben, A., and Gordon, J.: The relative importance of climate change and population growth for exposure to future extreme droughts, Clim. Change, 138, 1-2, 41-53, doi: 10.1007/s10584-016-1716-z, 2016.

Taylor, L.E., Stouffer, R.J., and Meehl, G.A.: An Overview of CMIP5 and the Experiment Design, B. Am. Meteorol. Soc., https://doi.org/10.1175/BAMS-D-11-00094.1, 2012.

UNFCCC Conference of the Parties: Adoption of the Paris Agreement, FCCC/CP/2015/10Add.1, 1-32, Paris, 2015.

Earth Syst. Dynam. Discuss., https://doi.org/10.5194/esd-2017-85
Manuscript under review for journal Earth Syst. Dynam.
Discussion started: 3 November 2017

Van Dijk, A.I.J.M., Beck, H.E., Crosbie, R.S., de Jeu, A.M., Liu, Y.Y., Podger, G.M., Timbal, B., and Viney, N.R.: The Millennium Drought in southeast Australia (2001-2009): Natural and human causes and implications for water resources, ecosystems, economy, and society, Water Resour. Res., 49, 1040-1057, doi:10.1002/wrcr.20123, 2013.

Wang, A.H., Lettenmaier, D.P., Sheffield, J.: Soil moisture drought in China, 1950-2006, J. Climate, 24, 3257-3271, doi: 10.1175/2011JCLI3733.1, 2011.

Wang, Z.L., Lin, L., Zhang, X.Y., Zhang, H., Liu, L.K., and Xu, Y.Y.: Scenario dependence of future changes in climate extremes under 1.5°C and 2°C global warming, Sci. Rep., 7:46432, doi:10.1038/srep46432, 2017.

Wells, N., Goddard, S., Hayes, M.J.: A self-calibrating palmer drought severity index, J. Clim., 17, 2335-2351, 2004.

Yevjevich, V., and Ingenieur, J.: An objective approach to definitions and investigations of continental hydrological drought, Water Resource Publ., Fort Collins, 1967.

Zhang, J., Sun, F.B., Xu, J.J., Chen, Y.N., Sang, Y.-F., and Liu, C.M.: Dependence of trends in and sensitivity of drought over China (1961-2013) on potential evaporation model, 43, 206-213, doi: 10.1002/2015GL067473, 2016.

Zuo, D.D., Hou, W., and Wang, W.X.: Sensitivity analysis of sample number of the drought descriptive model built by Copula function in southwest China, Acta Phys. Sin., 64(10), 100203, doi:10.7498/aps.64.100203,2015

Earth Syst. Dynam. Discuss., https://doi.org/10.5194/esd-2017-85
Manuscript under review for journal Earth Syst. Dynam.
Discussion started: 3 November 2017

Earth System Dynamics Discussions Open Access EGU

564 **Table 1:** Details of CMIP5 climate models applied in this study

565

Climate models	abbreviation	Horizontal Resolution	Future Scenarios
ACCESS1.0	ACCESS	1.300×1.900 degree	RCP4.5, RCP8.5
BCC_CSM1.1	BCC	2.813×2.791 degree	RCP4.5, RCP8.5
BNU-ESM	BNU	2.810×2.810 degree	RCP4.5, RCP8.5
CanESM23	CANESM	2.813×2.791 degree	RCP4.5, RCP8.5
CNRM-CM5	CNRM	1.406×1.401 degree	RCP4.5, RCP8.5
CSIRO Mk3.6.0	CSIRO	1.875×1.866 degree	RCP4.5, RCP8.5
GFDL CM3	GFDL	2.500×2.000 degree	RCP4.5, RCP8.5
INM-CM4.0	INM	2.000×1.500 degree	RCP4.5, RCP8.5
IPSL-CM5B-LR	IPSL	1.875×3.750 degree	RCP4.5, RCP8.5
MRI-CGCM3	MRI	1.125×1.125 degree	RCP4.5, RCP8.5
MIROC-ESM	MIROC	2.813×2.791 degree	RCP4.5, RCP8.5

Earth Syst. Dynam. Discuss., https://doi.org/10.5194/esd-2017-85
Manuscript under review for journal Earth Syst. Dynam.
Discussion started: 3 November 2017

Table 2: Definition of regions in this study, after IPCC (2012)

ID	abbreviation	Regional Representation
1	ALA	Alaska/Northwest Canada
2	CGI	East Canada, Greenland, Iceland
3	WNA	West North America
4	CNA	Central North America
5	ENA	East North America
6	CAM	Central America and Mexico
7	AMZ	Amazon
8	NEB	Northeastern Brazil
9	WSA	West Coast South America
10	SSA	Southeastern South America
11	NEU	Northern Europe
12	CEU	Central Europe
13	MED	Southern Europe and Mediterranean
14	SAH	Sahara
15	WAF	West Africa
16	EAF	East Africa
17	SAF	Southern Africa
18	NAS	North Asia
19	WAS	West Asia
20	CAS	Central Asia
21	TIB	Tibetan Plateau
22	EAS	East Asia
23	SAS	South Asia
24	SEA	Southeast Asia
25	NAU	North Australia
26	SAU	South Australia/New Zealand
27	GLOBE	Globe

Earth Syst. Dynam. Discuss., https://doi.org/10.5194/esd-2017-85
Manuscript under review for journal Earth Syst. Dynam.
Discussion started: 3 November 2017

Table 3: Changes in population exposure (including total, urban and rural population, mean ± standard deviation of multi-model projections, unit: million) to severe drought at the globe and in 27 world regions in the 1.5°C and 2°C warmer worlds relative to the baseline period (1985-2006) using the SSP1 population dataset

Regions	1.5°C warming			2.0°C warming		
	Total	Urban	Rural	Total	Urban	Rural
ALA	0.0±0.1	0.0±0.1	0.0±0.0	-0.0±0.1	0.0±0.1	0.0±0.0
CGI	0.1±0.1	0.1±0.1	0.0±0.0	0.0±0.1	0.1±0.1	0.0±0.0
WNA	0.6±1.6	1.8±0.9	-1.2±0.9	1.5±2.6	-1.4±1.1	0.1±0.1
CNA	5.3±8.2	4.5±6.6	0.8±1.7	3.6±5.1	7.8±4.2	0.4±1.0
ENA	4.9±11.6	5.1±10.1	-0.1±1.6	-0.5±6.4	12.3±6.5	-0.6±1.0
CAM	7.1±9.1	10.3±7.9	-3.2±2.2	4.5±6.7	14.8±5.5	-4.6±2.4
AMZ	3.3±2.7	3.9±2.4	-0.6±0.7	4.1±5.6	7.1±4.5	-0.3±1.2
NEB	2.8±3.4	4.7±2.4	-1.9±1.4	4.4±5.4	7.6±4.0	-1.7±1.6
WSA	4.2±4.3	4.1±3.8	0.1±1.6	4.2±4.4	5.8±3.8	0.0±0.5
SSA	5.3±5.2	7.3±4.4	-2.0±1.5	0.6±5.2	8.6±4.8	-2.3±1.5
NEU	3.6±3.9	5.0±3.1	-1.5±1.5	2.6±9.6	8.1±8.1	-2.0±1.8
CEU	12.2±10.5	16.4±8.5	-4.2±3.5	0.7±29.3	27.2±24.2	-5.8±5.2
MED	14.1±6.8	13.3±4.7	0.9±3.4	20.8±21.9	30.6±16.9	0.3±4.9
SAH	2.9±3.7	2.8±1.9	0.1±2.5	6.3±6.7	6.4±4.0	0.3±3.2
WAF	26.6±32.0	26.7±15.7	-0.1±18.0	62.6±78.1	61.9±53.0	-4.5±23.0
EAF	9.3±23.8	11.4±4.0	-2.1±20.9	43.1±33.0	28.0±13.0	-9.4±23.0
SAF	9.2±3.6	7.3±2.1	1.9±1.9	18.9±10.2	18.9±7.8	0.9±2.6
NAS	1.4±6.2	3.0±4.0	-1.6±2.4	-7.9±7.2	3.0±5.2	-2.4±2.4
WAS	11.5±12.5	14.9±7.8	-3.4±5.8	27.1±17.6	28.8±12.8	-3.9±6.0
CAS	7.9±12.3	5.7±6.1	2.2±6.4	4.5±6.7	14.8±5.5	1.2±3.5
TIB	0.9±4.1	0.6±1.6	0.3±2.7	-3.7±3.5	2.4±2.5	-1.0±2.1
EAS	41.5±33.9	44.3±20.6	-2.8±19.8	-17.5±58.1	57.2±41.3	-21.5±24.7
SAS	63.6±86.3	17.7±37.6	45.9±52.4	0.5±72.7	68.5±52.3	-23.1±26.9
SEA	19.4±22.6	19.9±17.0	-0.5±8.2	41.3±21.1	26.1±21.9	-17.2±8.4
NAU	0.1±0.1	0.1±0.1	0.0±0.0	0.2±0.3	0.2±0.3	0.0±0.1
SAU	1.0±1.1	1.1±1.0	-0.1±0.2	3.2±2.0	3.2±1.8	-0.1±0.2
GLOBE	259.3±238.1	232.6±124.8	26.7±119.0	245.8±331.1	468.3±228.0	-99.3±100.2

Table 4: Changes in population exposure (including total, urban and rural population, mean ± standard deviation of multi-model projections, unit: million) to severe drought at the globe and in 27 world regions in the 1.5°C and 2°C warmer worlds relative to the baseline period using the fixed SSP1 population in 2100 (at the end of the 21st century). The italic numbers in the brackets show the people affected solely by severe droughts under two future warming scenarios, which were calculated using the fixed SSP1 baseline population in 2000 (do not consider the population growth with the development of socioeconomics in the future)

Regions	1.5°C warming			2.0°C warming		
	Total	Urban	Rural	Total	Urban	Rural
ALA	0.0±0.1(*-0.0±0.1*)	0.0±0.1(*-0.0±0.1*)	0.0±0.0(*0.0±0.0*)	0.0±0.1(*0.0±0.1*)	0.0±0.1(*0.0±0.1*)	0.0±0.0(*0.0±0.0*)
CGI	0.1±0.1(*0.0±0.1*)	0.0±0.1(*0.0±0.0*)	0.0±0.0(*0.0±0.0*)	0.1±0.1(*0.0±0.1*)	0.0±0.1(*0.0±0.0*)	0.0±0.0(*0.0±0.0*)
WNA	0.2±1.1(*0.2±1.5*)	0.2±1.1(*0.2±0.6*)	0.0±0.0(*0.0±0.9*)	0.8±1.8(*1.1±2.3*)	0.8±1.7(*0.6±0.8*)	0.0±0.1(*0.5±1.5*)
CNA	4.9±10.9(*3.1±6.8*)	4.5±10.2(*2.2±5.0*)	0.4±0.7(*0.9±1.8*)	6.1±6.6(*3.8±4.1*)	5.6±6.2(*2.7±3.0*)	0.5±0.4(*1.1±1.1*)
ENA	3.0±17.0(*1.9±10.0*)	3.0±16.8(*1.3±8.2*)	0.1±0.2(*0.6±2.0*)	7.5±9.9(*3.4±4.8*)	7.4±9.8(*0.2±1.5*)	0.1±0.1(*0.1±1.3*)
CAM	2.3±7.8(*2.1±7.2*)	2.2±7.6(*0.6±4.0*)	0.1±0.2(*1.5±3.3*)	8.5±9.4(*7.8±8.6*)	8.2±9.12(*3.5±4.6*)	0.3±0.3(*4.3±4.3*)
AMZ	2.1±2.0(*2.0±2.1*)	1.9±1.9(*0.9±1.1*)	0.2±0.2(*1.1±1.1*)	4.6±4.3(*4.8±4.5*)	4.1±3.9(*1.6±1.8*)	0.5±0.6(*3.2±2.9*)
NEB	1.4±2.3(*2.0±3.1*)	1.3±2.1(*0.6±1.0*)	0.1±0.2(*1.4±2.1*)	3.8±3.6(*5.3±4.9*)	3.4±3.3(*1.4±1.5*)	0.4±0.3(*3.9±3.5*)
WSA	4.2±15.1(*2.3±3.4*)	4.2±14.1(*1.9±2.8*)	0.1±1.1(*0.5±0.7*)	13.0±17.9(*2.4±2.7*)	12.5±16.7(*1.8±2.2*)	0.5±1.3(*0.6±0.6*)
SSA	2.5±4.1(*2.6±4.3*)	2.5±4.1(*1.5±2.7*)	0.0±0.1(*1.2±1.9*)	3.5±3.8(*3.9±4.3*)	3.4±3.7(*1.9±2.1*)	0.1±0.1(*2.1±2.4*)
NEU	3.0±4.7(*2.4±3.7*)	3.0±4.5(*1.5±2.2*)	0.1±0.2(*0.9±1.5*)	4.3±9.7(*3.5±7.7*)	4.2±9.5(*2.2±4.8*)	0.1±0.3(*1.3±2.9*)
CEU	10.5±8.7(*12.0±10.3*)	10.1±8.4(*6.4±5.7*)	0.4±0.3 (*5.5±4.7*)	18.4±24.0(*22.6±28.2*)	17.7±23.0(*11.5±14.9*)	0.8±1.0(*11.1±13.3*)
MED	9.8±6.5(*9.0±6.0*)	9.2±6.1(*3.6±2.2*)	0.5±0.5(*5.4±4.1*)	22.5±17.8(*21.1±16.5*)	21.2±16.7(*8.1±6.6*)	1.3±1.1(*13.0±9.9*)
SAH	-0.3±7.0(*0.2±3.6*)	0.0±5.5(*0.5±1.6*)	-0.3±1.6(*-0.3±2.5*)	1.7±9.1(*1.4±4.7*)	1.8±7.2(*1.3±2.3*)	-0.2±2.1(*0.1±3.2*)
WAF	2.7±71.7(*1.9±22.5*)	2.9±66.3(*0.7±3.2*)	-0.2±5.5(*1.2±19.5*)	14.3±109.5(*6.3±34.6*)	14.0±101.2(*1.9±5.1*)	0.3±8.4(*4.4±26.7*)
EAF	-23.7±58.0(*-9.2±23.5*)	-20.7±51.1(*-1.4±3.1*)	-3.0±7.0(*-7.8±20.6*)	-26.3±63.8(*-10.2±26.3*)	-22.6±56.2(*-1.8±3.0*)	-3.7±7.7(*-8.4±23.5*)
SAF	5.8±4.2(*3.2±2.1*)	5.2±3.8(*1.1±0.6*)	0.6±0.5(*2.1±1.8*)	12.0±9.0(*7.3±5.0*)	11.0±8.2(*2.9±1.5*)	1.0±0.8(*4.4±3.8*)
NAS	1.1±4.1(*1.7±6.3*)	1.1±3.7(*0.8±3.3*)	0.0±0.4(*0.9±3.0*)	1.1±5.1(*1.7±7.8*)	1.0±4.6(*0.6±4.1*)	0.1±0.5(*1.1±3.7*)
WAS	4.2±15.1(*4.7±10.4*)	4.2±14.1(*1.5±3.0*)	0.1±1.1(*3.2±7.6*)	13.0±17.9(*11.8±12.0*)	12.5±16.7(*3.8±3.5*)	0.5±1.3(*8.0±8.8*)
CAS	1.7±15.3(*1.6±10.6*)	1.0±14.0(*0.5±4.7*)	0.7±1.5(*1.1±6.1*)	7.0±9.4(*5.3±6.6*)	5.5±8.8(*1.7±3.2*)	1.5±1.0(*3.6±3.6*)
TIB	0.1±3.2(*0.3±2.6*)	0.0±2.8(*-0.0±1.2*)	0.1±0.6(*0.3±2.5*)	0.6±2.9(*1.0±3.4*)	0.4±2.6(*0.2±1.2*)	0.2±0.7(*0.8±2.5*)
EAS	17.3±17.8(*31.6±34.1*)	16.6±16.2(*16.4±15.6*)	0.7±1.8(*15.3±19.9*)	24.8±32.8(*46.2±64.2*)	24.0±30.0(*22.8±26.0*)	0.9±3.0(*23.4±39.3*)
SAS	-15.9±68.8(*-12.8±62.4*)	-14.9±61.3(*-7.7±34.9*)	-1.0±8.1(*-5.2±31.0*)	-35.9±52.6(*-31.9±47.7*)	-32.3±47.1(*-18.3±27.6*)	-3.6±6.0(*-13.6±24.3*)
SEA	1.0±16.1(*0.4±16.2*)	0.8±15.1(*-0.1±9.1*)	0.2±1.2(*0.5±8.5*)	1.5±14.4(*1.0±15.5*)	1.4±13.2(*0.7±7.2*)	0.1±1.5 (*0.4±9.3*)
NAU	0.1±0.1(*0.1±0.1*)	0.1±0.1(*0.0±0.0*)	0.0±0.0(*0.0±0.1*)	0.2±0.3(*0.1±0.2*)	01±0.2(*0.0±0.1*)	0.0±0.0 (*0.1±0.1*)
SAU	0.8±1.7(*0.3±0.8*)	0.8±17(*0.3±0.6*)	0.0±0.0(*0.1±0.2*)	2.4±2.1(*1.1±1.0*)	2.4±2.1(*0.8±0.7*)	0.0±0.0(*0.3±0.3*)
GLOBE	38.6±272.7(*63.8±195.9*)	38.7±247.1(*33.3±86.6*)	0.0±26.1(*30.5±113.6*)	100.3±323.9(*122.4±249.9*)	99.1±295.9(*55.4±101.8*)	1.5±28.5(*67.0±150.7*)

Earth Syst. Dynam. Discuss., https://doi.org/10.5194/esd-2017-85
Manuscript under review for journal Earth Syst. Dynam.
Discussion started: 3 November 2017

Earth System Dynamics
Discussions
Open Access

Figure captions:

Figure 1: Definition of the baseline period, 1.5^{o}C and 2^{o}C worlds based on CMIP5 GCM-simulated changes in global mean temperature (GMT, relative to the pre-industrial levels: 1850-1900). The dark blue and dark yellow shadows indicate the 25th and 75th percentiles of multi-model simulated GMT for RCP 4.5 and RCP 8.5 scenarios, respectively. Both the multi-model ensemble mean and percentiles shown in the figure are smoothed using a moving average approach in a 20-year window

Figure 2: Palmer Drought Severity Index (PDSI)-based drought characteristics definition through the run theory

Figure 3: Changes in multi-model ensemble mean PDSI (i) and model consistency (ii) on a spatial resolution of 0.5^{o} × 0.5^{o}, (a) from the baseline period to 1.5^{o}C, (b) from the baseline period to 2^{o}C and (c) from 2^{o}C to 1.5^{o}C. Robustness of projections increases with higher model consistency and vice-versa. The dark-gray boxes show the world regions adopted by IPCC (2012), which are labeled in (a)(i) using the ID numbers defined in Table 2. Legend in (a)(i) applies to (b)(i) and (c)(i); legend in (a)(ii) applies to (b)(ii) and (c)(ii).

Figure 4: Multi-model projected PDSI at the globe (66^{o}N-66^{o}S) and in 27 world regions for the baseline period, 1.5^{o}C and 2^{o}C warmer worlds. The projected uncertainty of multiple climate models is shown through box plots for each region and for each period

Figure 5: Changes in multi-model ensemble mean drought duration (i) and model consistency (ii) on a spatial resolution of 0.5^{o} × 0.5^{o}, (a) from the baseline period to 1.5^{o}C, (b) from the baseline period to 2^{o}C and (c) from 2^{o}C to 1.5^{o}C. The dark-gray boxes show the regions adopted by IPCC (2012), which are labeled in (a)(i) using the ID numbers defined in Table 2. Legend in (a)(i) applies to (b)(i) and (c)(i); legend in (a)(ii) applies to (b)(ii) and (c)(ii).

Figure 6: Multi-model projected drought duration at the globe (66^{o}N-66^{o}S) and in 27 world regions for the baseline period, 1.5^{o}C and 2^{o}C warmer worlds. The projected uncertainty of multiple climate models is shown through box plots for each region and for each period

Figure 7: Changes in multi-model ensemble mean drought intensity (i) and model consistency (ii) on a spatial resolution of 0.5^{o} × 0.5^{o}, (a) from the baseline period to 1.5^{o}C, (b) from the baseline period to 2^{o}C and (c) from 2^{o}C to 1.5^{o}C. The dark-gray boxes show the regions adopted by IPCC (2012), which are labeled in (a)(i) using the ID numbers defined in Table 2. Legend in (a)(i) applies to (b)(i) and (c)(i); legend in (a)(ii) applies to (b)(ii) and (c)(ii).

Figure 8: Multi-model projected drought intensity at the globe (66^{o}N-66^{o}S) and in 27 world regions for the baseline period, 1.5^{o}C and 2^{o}C warmer worlds. The projected uncertainty of multiple climate models is shown through box plots for each region and for each period

Figure 9: Changes in multi-model ensemble mean drought severity (i) and model consistency (ii) on a spatial resolution of 0.5^{o} × 0.5^{o}, (a) from the baseline period to 1.5^{o}C, (b) from the baseline period to 2^{o}C and (c) from 2^{o}C to 1.5^{o}C. The dark-gray boxes show the regions adopted by IPCC (2012), which are labeled in (a)(i) using the ID numbers defined in Table 2. Legend in (a)(i) applies to (b)(i) and (c)(i); legend in (a)(ii) applies to (b)(ii) and (c)(ii).

Figure 10: Multi-model projected drought severity at the globe (66^{o}N-66^{o}S) and in 27 world regions for the baseline period, 1.5^{o}C and 2^{o}C warmer worlds. The projected uncertainty of multiple climate models is shown through box plots for each region and for each period

Figure 11: Multi-model projected frequency (Freq.) and affected total population (Pop., million) of severe drought (pdsi < -3) at the globe and in 27 world regions for the baseline period (black),

Earth Syst. Dynam. Discuss., https://doi.org/10.5194/esd-2017-85
Manuscript under review for journal Earth Syst. Dynam.
Discussion started: 3 November 2017

Earth System Dynamics Discussions

1.5°C (orange) and 2°C (red) warmer worlds. The projected uncertainties (standard deviation of multiple-model results) of multiple climate models are shown by error bars (horizontal and vertical)

Figure 12: Multi-model projected frequency (Freq.) and affected urban population (Pop., million) of severe drought (pdsi < -3) at the globe and in 27 regions for the baseline period (black), 1.5 °C (orange) and 2 °C (red) warmer worlds. The projected uncertainties (standard deviation of multiple-model results) of multiple climate models are shown by error bars (horizontal and vertical)

Figure 13: Multi-model projected frequency (Freq.) and affected rural population (Pop., million) of severe drought (pdsi < -3) at the globe and in 27 regions for the baseline period (black), 1.5 °C (orange) and 2 °C (red) warmer worlds. The projected uncertainties (standard deviation of multiple-model results) of multiple climate models are shown by error bars (horizontal and vertical)

Earth Syst. Dynam. Discuss., https://doi.org/10.5194/esd-2017-85
Manuscript under review for journal Earth Syst. Dynam.
Discussion started: 3 November 2017

Figure 1: Definition of the baseline period, 1.5°C and 2°C warmer worlds based on CMIP5 GCM-simulated changes in global mean temperature (GMT, relative to the pre-industrial levels: 1850-1900). The dark blue and dark yellow shadows indicate the 25th and 75th percentiles of multi-model simulated GMT for RCP 4.5 and RCP 8.5 scenarios, respectively. Both the multi-model ensemble mean and percentiles shown in the figure are smoothed using a moving average approach in a 20-year window

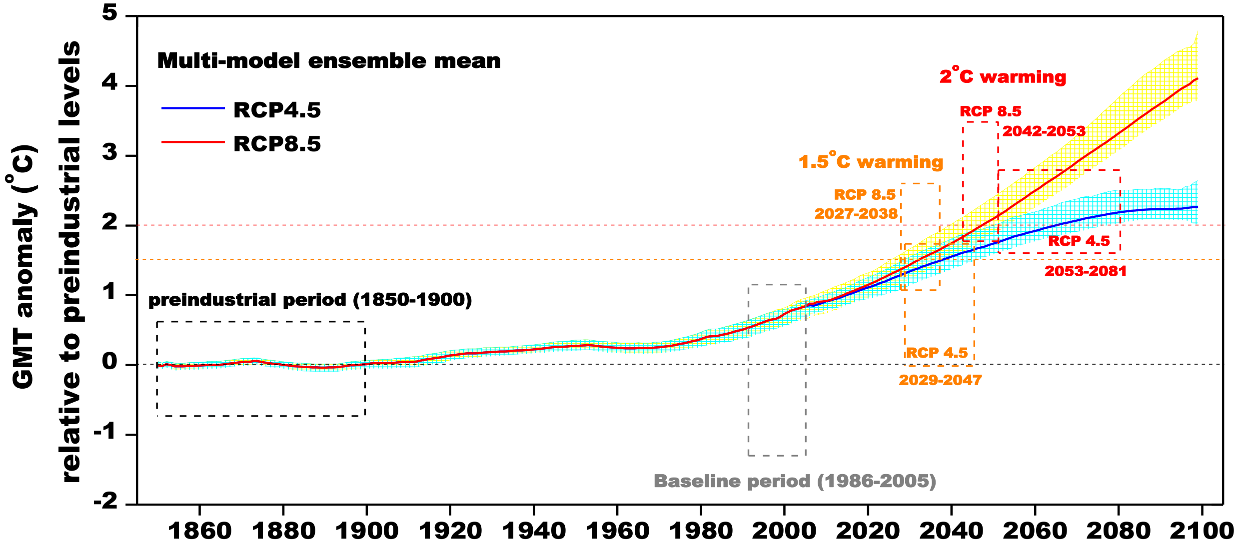

Earth Syst. Dynam. Discuss., https://doi.org/10.5194/esd-2017-85
Manuscript under review for journal Earth Syst. Dynam.
Discussion started: 3 November 2017

Earth System Dynamics
Open Access
Discussions

Figure 2: Palmer Drought Severity Index (PDSI)-based drought characteristics definition through the run theory

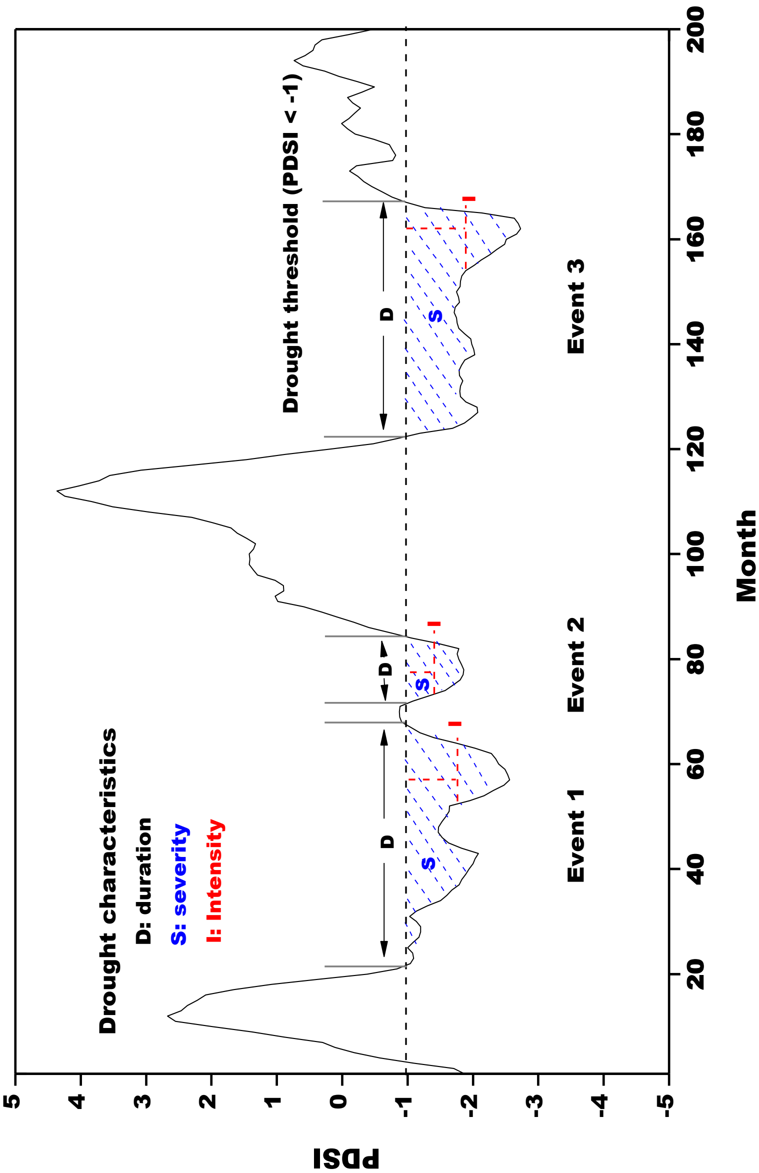

Earth Syst. Dynam. Discuss., https://doi.org/10.5194/esd-2017-85
Manuscript under review for journal Earth Syst. Dynam.
Discussion started: 3 November 2017

Figure 3: Changes in multi-model ensemble mean PDSI (i) and model consistency (ii) on a spatial resolution of $0.5^o \times 0.5^o$, (a) from the baseline period to 1.5^oC, (b) from the baseline period to 2^oC and (c) from 2^oC to 1.5^oC. Robustness of projections increases with higher model consistency and vice-versa. The dark-gray boxes show the world regions adopted by IPCC (2012), which are labeled in (a)(i) using the ID numbers defined in Table 2. Legend in (a)(i) applies to (b)(i) and (c)(i); legend in (a)(ii) applies to (b)(ii) and (c)(ii).

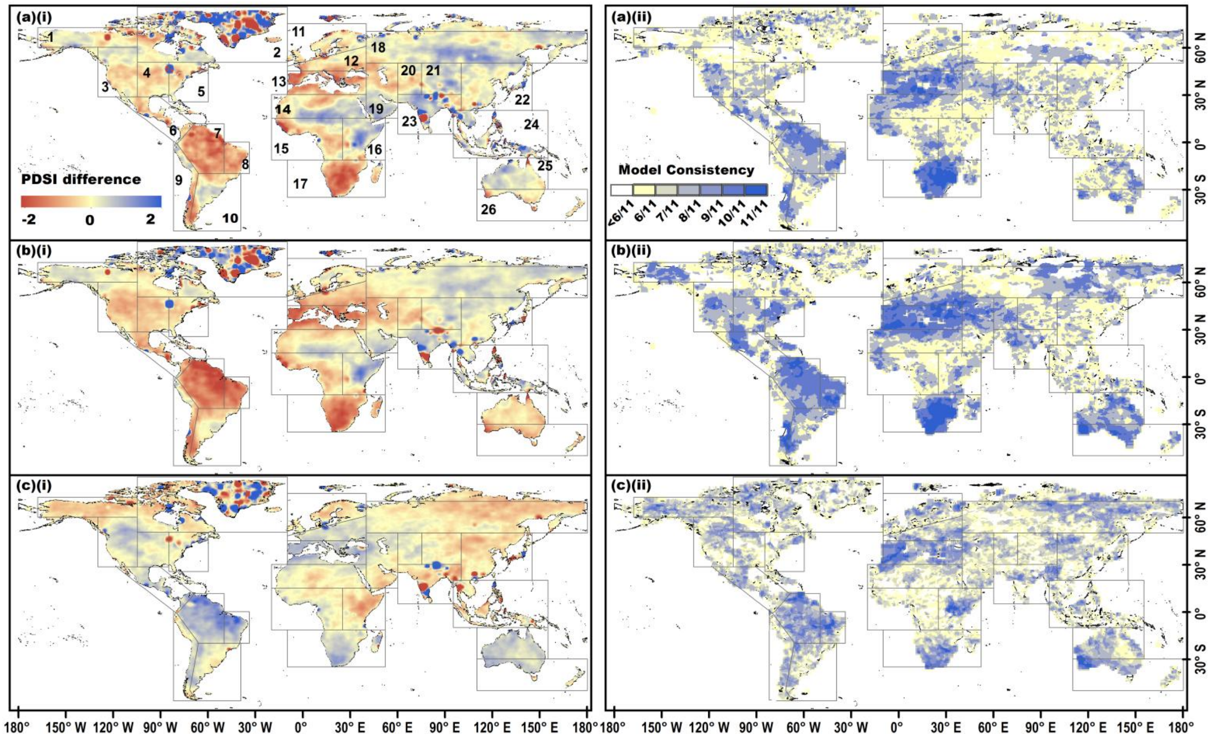

Figure 4: Multi-model projected PDSI at the globe (66°N-66°S) and in 27 world regions for the baseline period, 1.5°C and 2°C warmer worlds. The projected uncertainty of multiple climate models is shown through box plots for each region and for each period

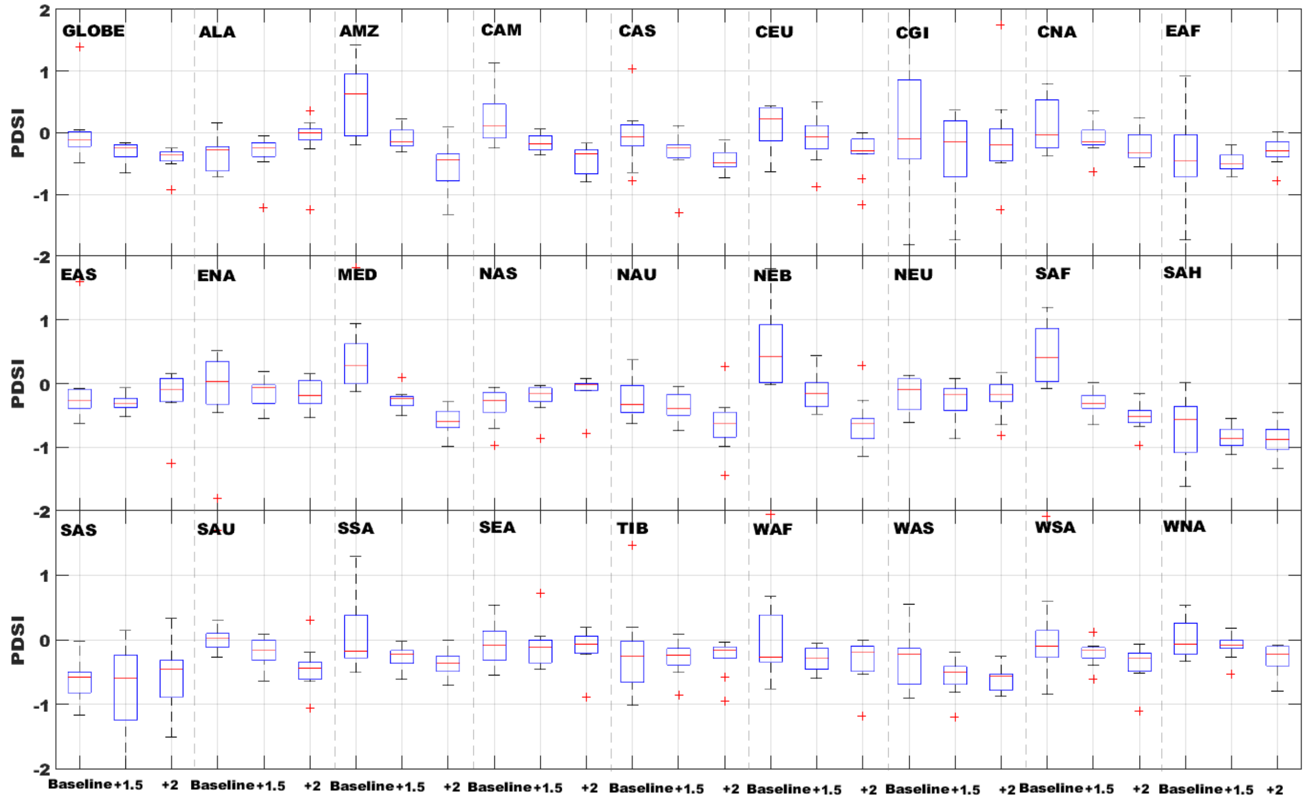

Earth Syst. Dynam. Discuss., https://doi.org/10.5194/esd-2017-85
Manuscript under review for journal Earth Syst. Dynam.
Discussion started: 3 November 2017

Figure 5: Changes in multi-model ensemble mean drought duration (i) and model consistency (ii) on a spatial resolution of 0.5° × 0.5°, (a) from the baseline period to 1.5°C, (b) from the baseline period to 2°C and (c) from 2°C to 1.5°C. The dark-gray boxes show the regions adopted by IPCC (2012), which are labeled in (a)(i) using the ID numbers defined in Table 2. Legend in (a)(i) applies to (b)(i) and (c)(i); legend in (a)(ii) applies to (b)(ii) and (c)(ii).

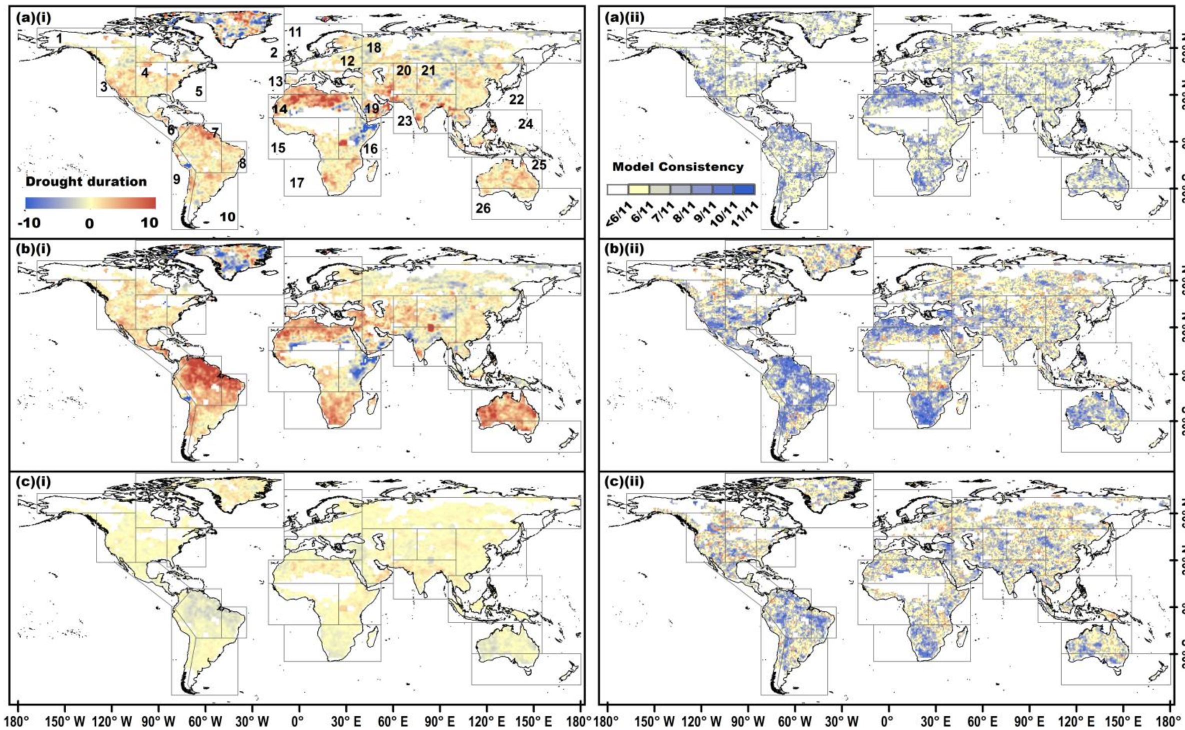

Figure 6: Multi-model projected drought duration at the globe (66°N-66°S) and in 27 regions for the baseline period, 1.5°C and 2°C warmer worlds. The projected uncertainty of multiple climate models is shown through box plots for each region and for each period

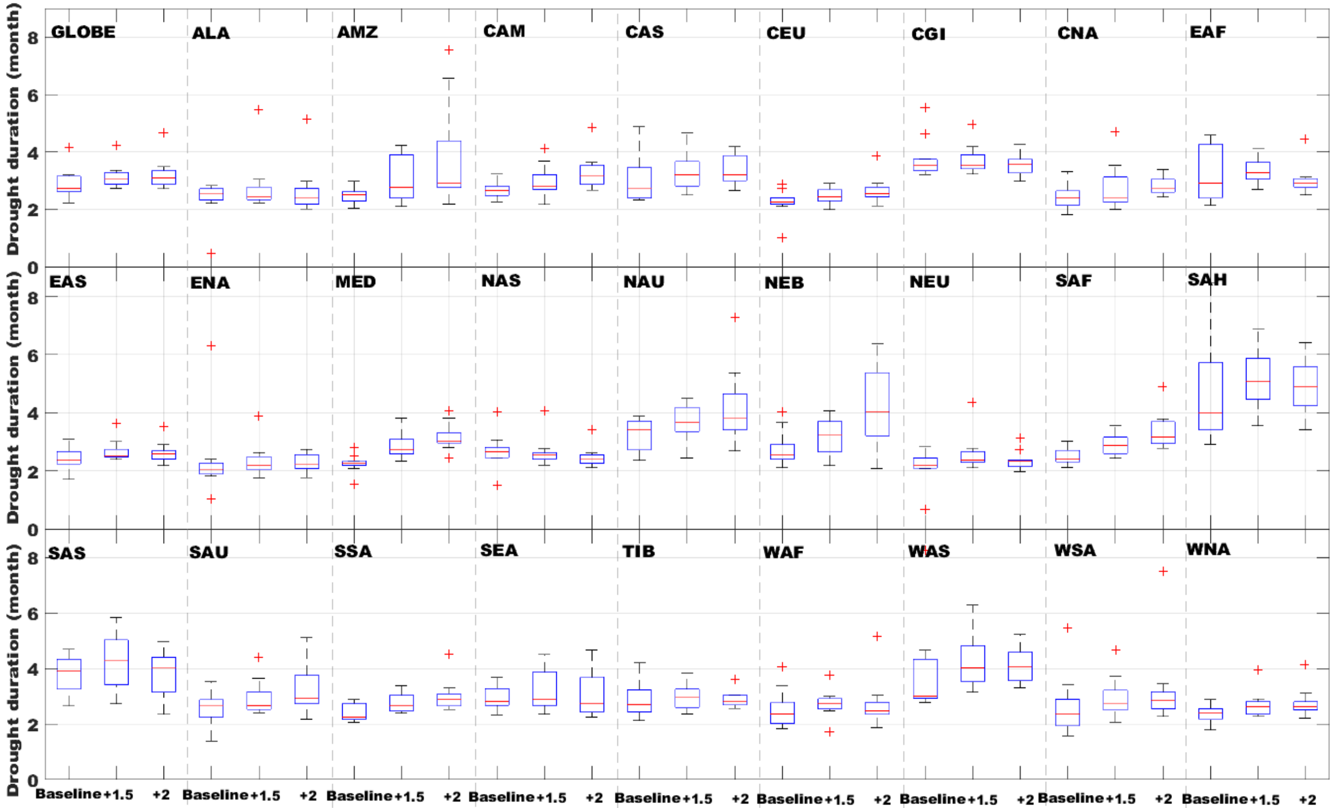

Earth Syst. Dynam. Discuss., https://doi.org/10.5194/esd-2017-85
Manuscript under review for journal Earth Syst. Dynam.
Discussion started: 3 November 2017

Figure 7: Changes in multi-model ensemble mean drought intensity (i) and model consistency (ii) on a spatial resolution of 0.5°× 0.5°, (a) from the baseline period to 1.5°C, (b) from the baseline period to 2°C and (c) from 2°C to 1.5°C. The dark-gray boxes show the regions adopted by IPCC (2012), which are labeled in (a)(i) using the ID numbers defined in Table 2. Legend in (a)(i) applies to (b)(i) and (c)(i); legend in (a)(ii) applies to (b)(ii) and (c)(ii).

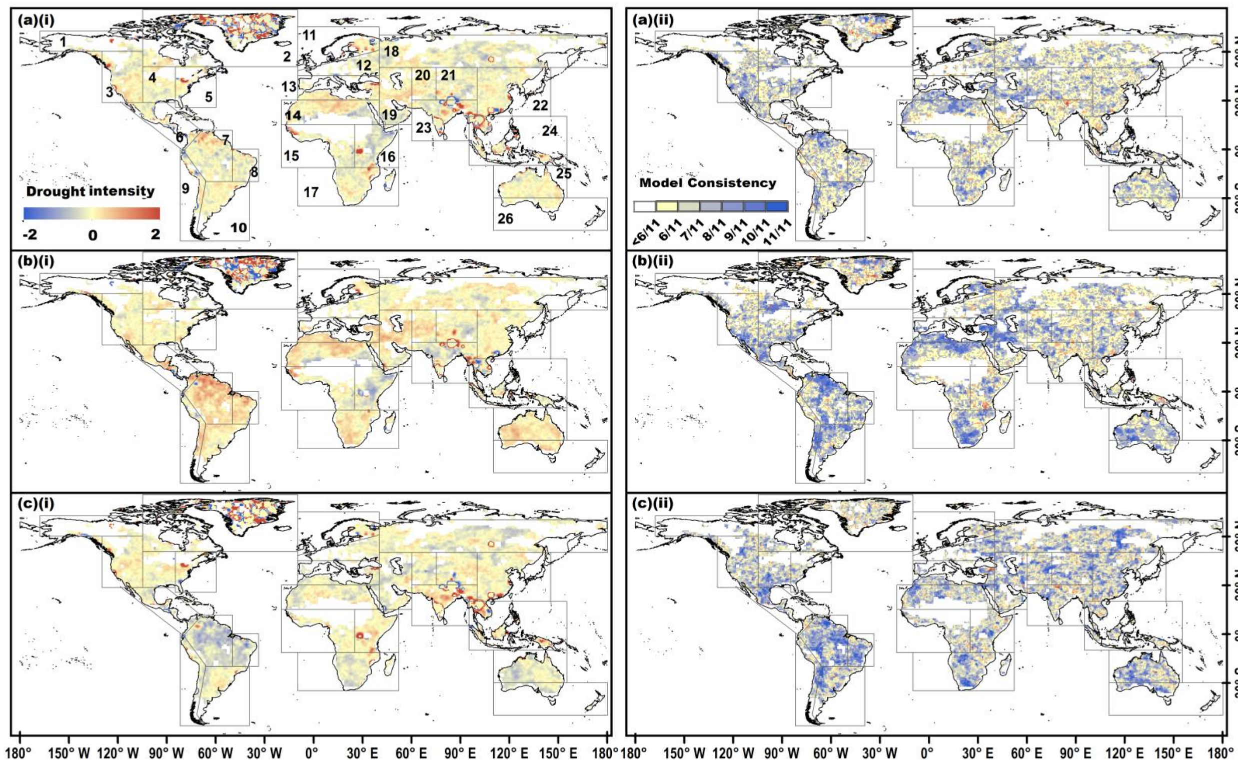

Earth Syst. Dynam. Discuss., https://doi.org/10.5194/esd-2017-85
Manuscript under review for journal Earth Syst. Dynam.
Discussion started: 3 November 2017

Earth System Dynamics
Open Access
Discussions

Figure 8: Multi-model projected drought intensity at the globe (66°N-66°S) and in 27 regions for the baseline period, 1.5°C and 2°C warmer worlds. The projected uncertainty of multiple climate models is shown through box plots for each region and for each period

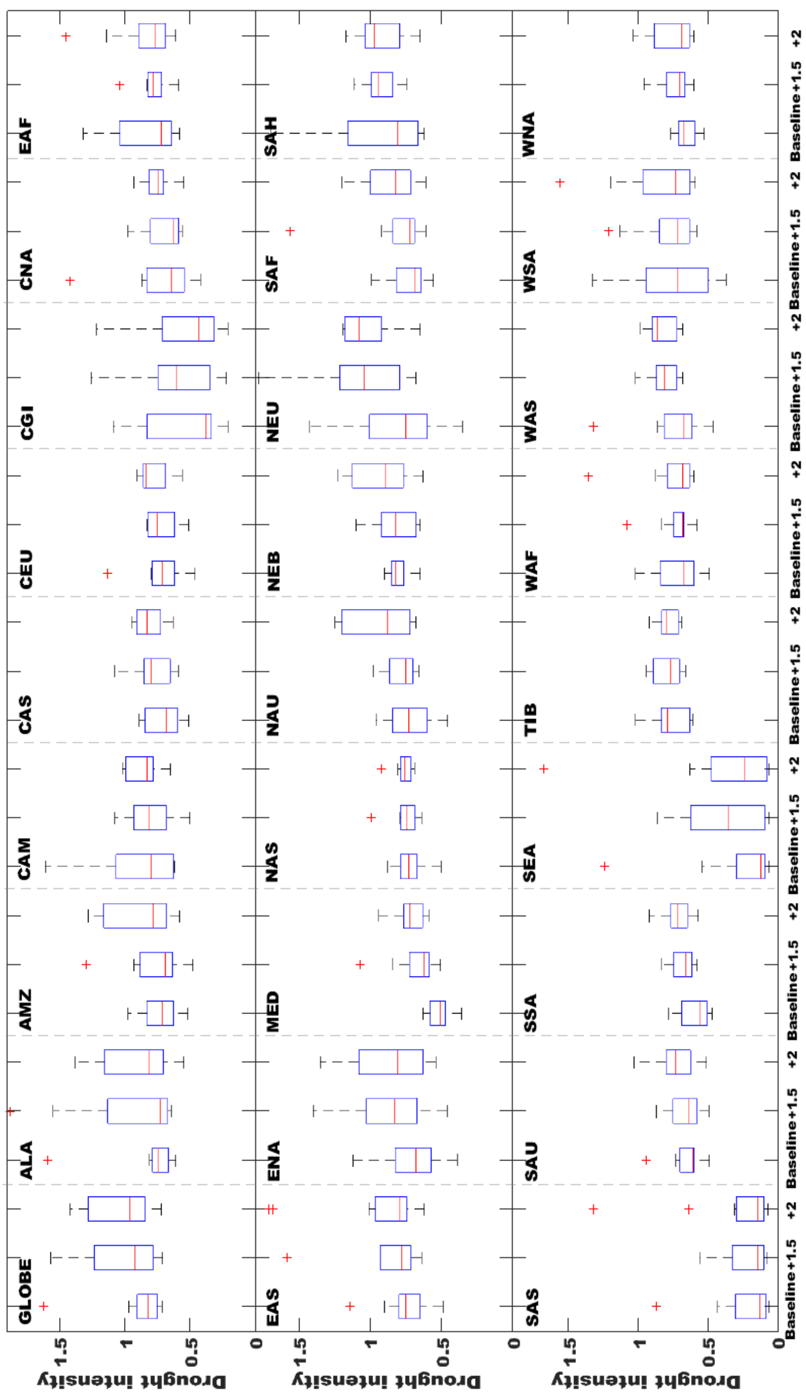

Figure 9: Changes in multi-model ensemble mean drought severity (i) and model consistency (ii) on a spatial resolution of 0.5° × 0.5°, (a) from the baseline period to 1.5°C, (b) from the baseline period to 2°C and (c) from 2°C to 1.5°C. The dark-gray boxes show the regions adopted by IPCC (2012), which are labeled in (a)(i) using the ID numbers defined in Table 2. Legend in (a)(i) applies to (b)(i) and (c)(i); legend in (a)(ii) applies to (b)(ii) and (c)(ii).

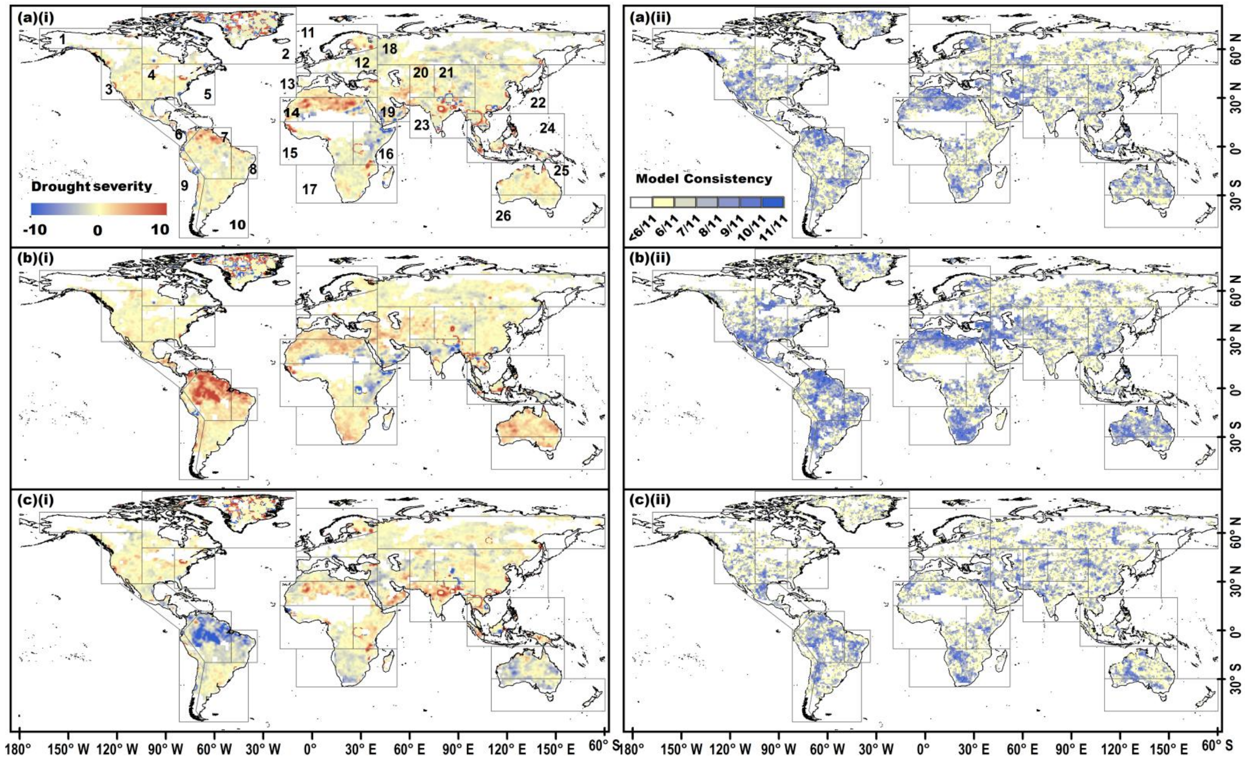

Earth Syst. Dynam. Discuss., https://doi.org/10.5194/esd-2017-85
Manuscript under review for journal Earth Syst. Dynam.
Discussion started: 3 November 2017

Earth System Dynamics
Discussions

Figure 10: Multi-model projected drought severity at the globe (66°N-66°S) and in 27 regions for the baseline period, 1.5°C and 2°C warmer worlds. The projected uncertainty of multiple climate models is shown through box plots for each region and for each period

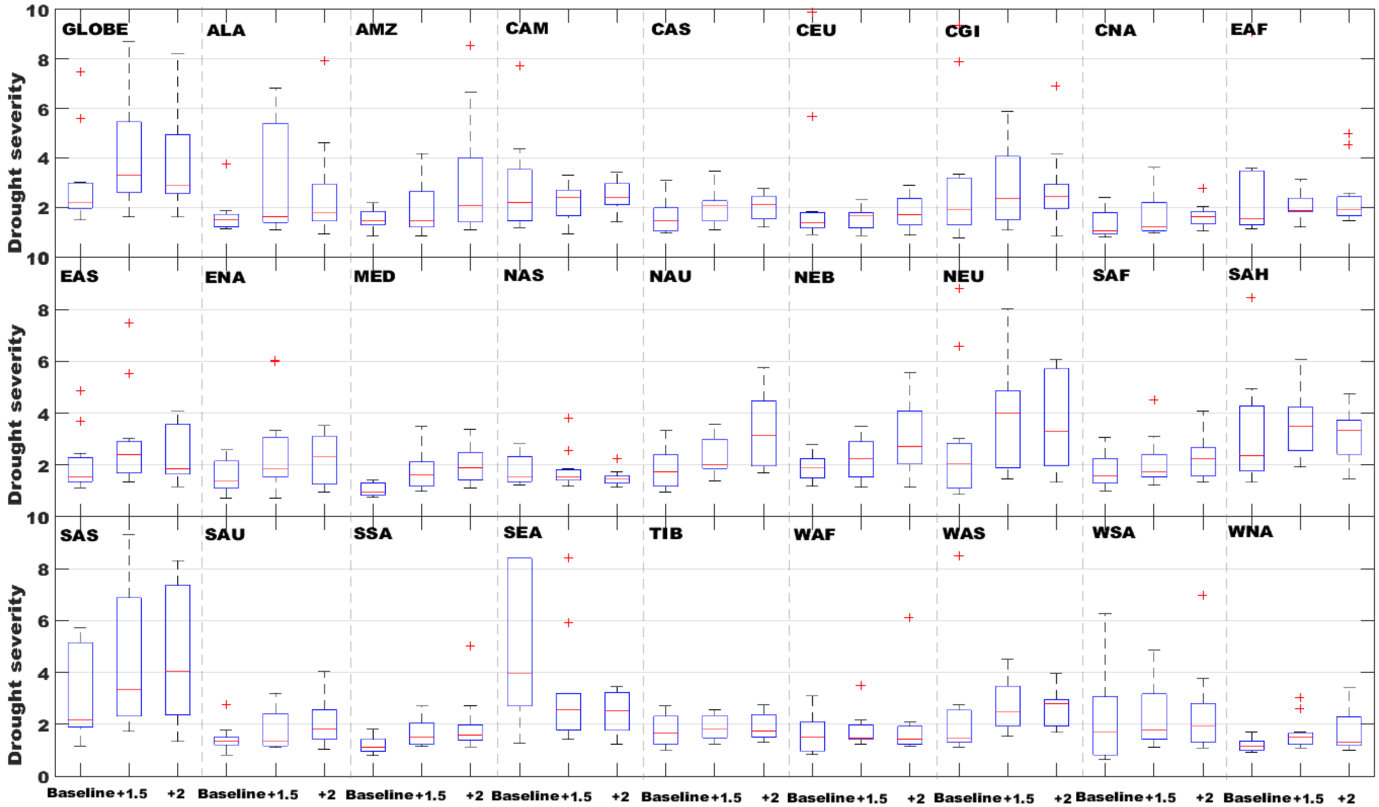

Earth Syst. Dynam. Discuss., https://doi.org/10.5194/esd-2017-85
Manuscript under review for journal Earth Syst. Dynam.
Discussion started: 3 November 2017

Earth System Dynamics
Open Access
Discussions

Figure 11: Multi-model projected frequency (Freq.) and affected total population (Pop., million) of severe drought (pdsi < -3) at the globe and in 27 regions for the baseline period (black), 1.5°C (orange) and 2°C (red) warmer worlds. The projected uncertainties (standard deviation of multiple-model results) of multiple climate models are shown by error bars (horizontal and vertical)

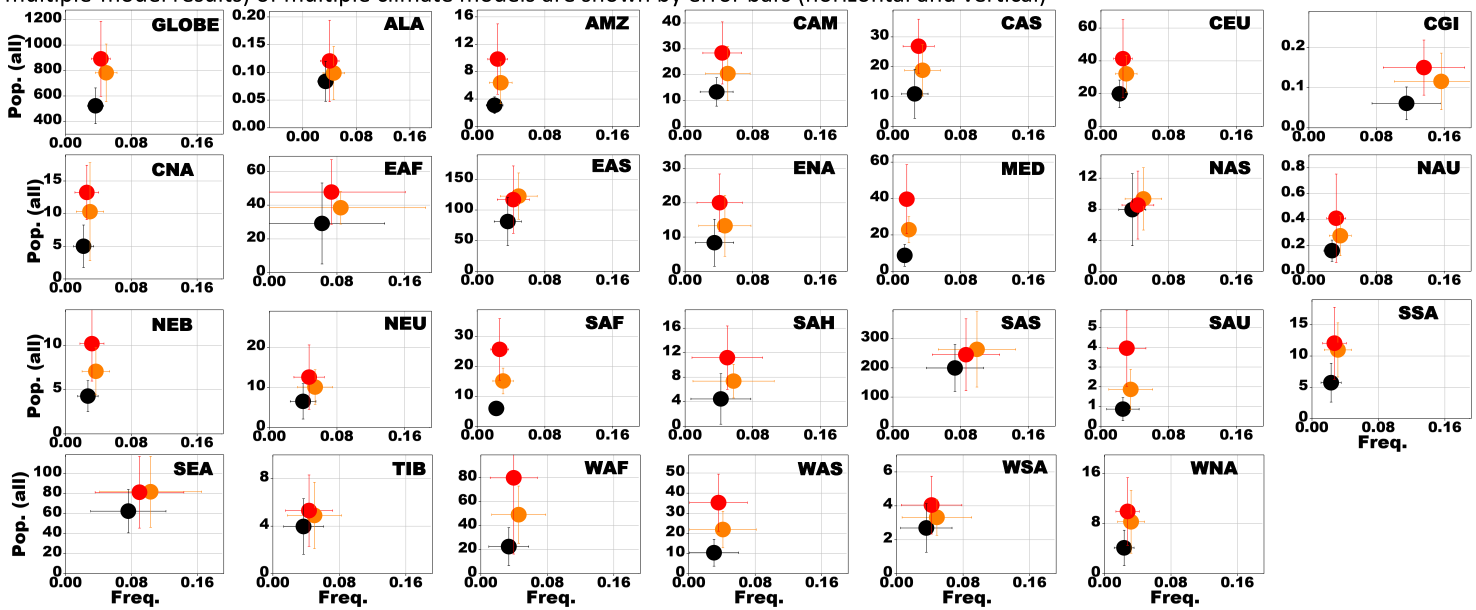

Earth Syst. Dynam. Discuss., https://doi.org/10.5194/esd-2017-85
Manuscript under review for journal Earth Syst. Dynam.
Discussion started: 3 November 2017

Earth System Dynamics
Discussions

Figure 12: Multi-model projected frequency (Freq.) and affected urban population (Pop., million) of severe drought (pdsi < -3) at the globe and in 27 regions for the baseline period (black), 1.5°C (orange) and 2°C (red) warmer worlds. The projected uncertainties (standard deviation of multiple-model results) of multiple climate models are shown by error bars (horizontal and vertical)

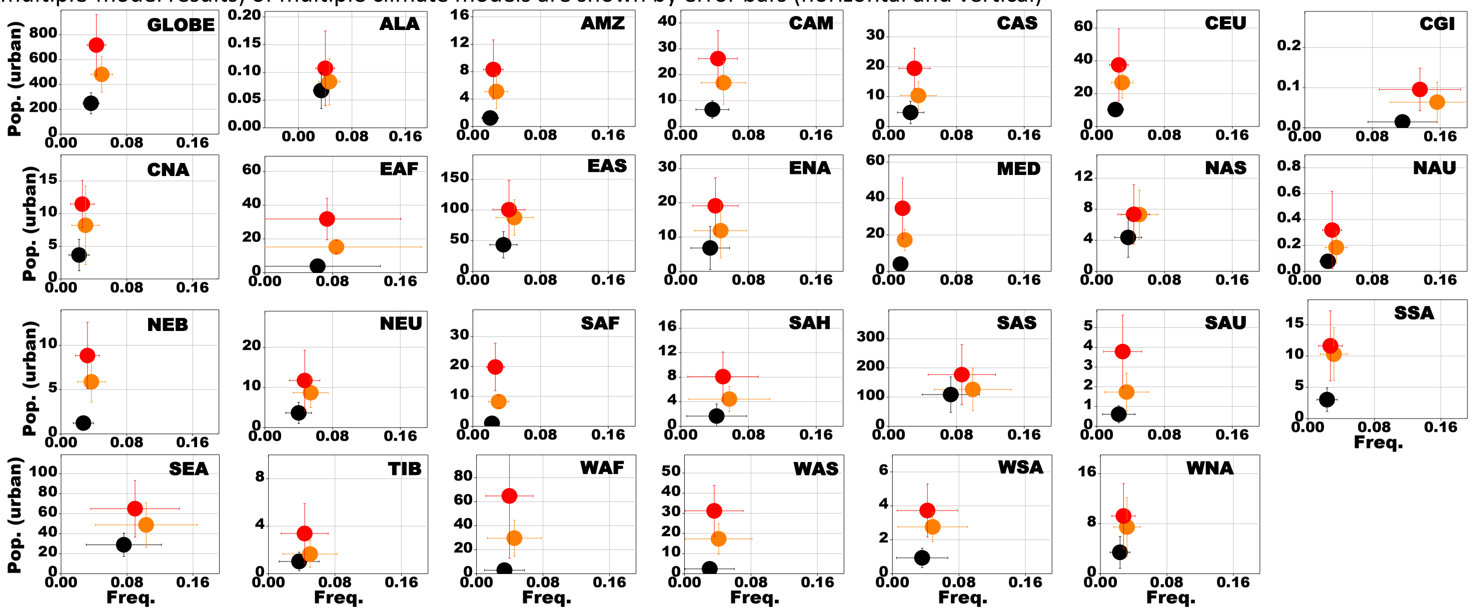

Earth Syst. Dynam. Discuss., https://doi.org/10.5194/esd-2017-85
Manuscript under review for journal Earth Syst. Dynam.
Discussion started: 3 November 2017

Earth System Dynamics
Discussions

Figure 13: Multi-model projected frequency (Freq.) and affected rural population (Pop., million) of severe drought (pdsi < -3) at the globe and in 27 regions for the baseline period (black), 1.5°C (orange) and 2°C (red) warmer worlds. The projected uncertainties (standard deviation of multiple-model results) of multiple climate models are shown by error bars (horizontal and vertical)